Politecnico di Torino

Department of Environment,
Land and Infrastructure Engineering

Master of Science in Georesources
and Geoenergy Engineering

Design of a Plant for Sulfur Oxides Production and Recovery

Candidate:

Mehran Moazeni Targhi

Supervisors:

Prof. Fabio Alessandro Deorsola
Prof. Samir Bensaid

July 2026

Abstract

The purpose of this study is to provide a sound design for the production and recovery of sulfur dioxide. The plant is simulated and analyzed by Aspen Plus. In the simulation stage, the reaction behavior, heat recovery, and operational sensitivity are considered. This involves the combustion of liquid sulfur and air in a furnace, followed by heat recovery stages. In the combustion stage, a high-temperature gas is produced and cooled with water in liquid, vapor, and two-phase states. The main objective of this work is to develop a complete process model that represents plant configuration and outlet conditions to assess the impact of key operating parameters on the overall system performance.

The simulation was carried out in a steady-state flowsheet that includes reactors and multiple heat exchangers (as the furnace), a separator–reboiler vessel, and other equipment such as pumps, valves, and control elements. The heat recovery system consists of six heat exchangers in series within the furnace. After the combustion, the temperature of the process gas is reduced from approximately 1700 °C to 266 °C. A Separator (Reboiler) unit was modelled with a heating coil to ensure proper heat balance in the system. To improve energy efficiency, a heat recovery scheme was considered, and the furnace outlet stream was simulated to preheat the inlet air or the feed water. This enhances the thermal integration of the process and reduces the requirement for external heating utilities.

Design specifications were imposed on the inlet streams of the economizer and the superheater to help maintain the critical operating conditions. In the model, stream split fractions were modified to match the target outlet stream conditions, with mass and energy balance for the entire system. A sensitivity analysis was performed to study the effects of inlet air flow rate, humidity, oxygen purity, and temperature on the process performance. The influence of these parameters was studied on the selected variables with particular attention to the formation of SO_3, H_2SO_4, and acid dew point temperature. Results show that humidity and temperature affect secondary reaction pathways that are directly related to corrosion and operational stability.

Table of Contents

Table of Figures

Table of Tables

1. Introduction

Sulfur oxides, especially sulfur dioxide (SO_2) and sulfur trioxide (SO_3), are key compounds in large-scale industrial chemical processes. One of their main applications is the production of sulfuric acid, which remains among the most widely produced inorganic chemicals worldwide and is often used as an indicator of industrial development and economic activity [1], [2]. In industrial applications, sulfur dioxide is typically produced by burning elemental sulfur in dry air. Depending on the process configuration and the desired product recovery route, it can then be further oxidized to sulfur trioxide [2], [3].

The production of Sulfur oxides is important not only from a manufacturing perspective but also for environmental impact and process design. Sulfur dioxide emissions are well known as major contributors to air pollution, acid rain, and overall environmental degradation [4], [5]. For this reason, the design of sulfur oxide plants must address several objectives, including efficient production, effective control, and recovery of sulfur-containing emissions. Consequently, modern industrial systems are typically configured to integrate reaction, heat recovery, gas cooling, and separation stages within a single process.

The most important equipment in the sulfur dioxide production is the furnace. In this equipment, the reaction between liquid sulfur and air occurs. The result is a high-temperature gas stream that mostly consists of sulfur dioxide. Other reactions may occur in the cooling stage. Specifically, a small fraction of SO_2 can be transformed into SO_3. If the inlet air contains water content, the produced SO_3 can subsequently react with water content to produce sulfuric acid [2], [6].

Energy integration is an important part of sulfur oxide plant design. The combustion section produces a very hot gas stream, and a large amount of energy would be lost if it were not recovered. For this reason, waste heat boilers and heat exchangers are typically used to capture part of this energy and convert it into steam. This steam can then be reused within the plant, exported as a utility stream, and used to generate electricity [2], [7].

Sulfuric acid formation can alter the process behavior. It affects not only the composition of the stream but also increases the risk of corrosion and the accumulation of liquid in different parts of the equipment. Sulfuric acid formation affects the performance of

downstream separators and recovery drums. For this reason, it is important to monitor how temperature, moisture content, and sulfur oxide conversion interact during the cooling stage [6].

The purpose of this thesis is to provide a reliable design for sulfur oxide production and energy recovery. The main focus is to emphasize the sulfur furnace, heat recovery network, and cooling section. Aspen Plus is employed to simulate this process. Operating variables such as furnace temperature, feed moisture content, and heat recovery are considered, and their effect on the formation and recovery of SO_2, SO_3, and H_2SO_4 is discussed. Another aim of this thesis is to develop a technically feasible and thermally integrated process design while providing a better understanding of the governing chemical and thermodynamic behavior of sulfur oxide systems.

Industrial production of sulfur oxides depends on a variety of sulfur-containing raw materials. The choice of these materials depends on the cost of the process, the availability of local resources, the process integration, and the intended use of the product. Producing sulfur dioxide from elemental sulfur is a common approach in modern sulfuric acid plants [1].

Sulfur oxides are produced from sulfur-containing materials, including elemental sulfur, pyrite (FeS_2), sulfide ores of nonferrous metals, waste sulfuric acid streams, sulfate minerals, gypsum and anhydrite, hydrogen sulfide-containing gases, and flue gases from burning fossil fuels. These materials differ significantly in sulfur content, impurity profile and processing route, which directly affects plant design and recovery strategy [1].

1.1. Physical and chemical properties of SO_2

Sulfur dioxide (SO_2) is a colorless gas with a sharp, irritating odor that is readily detected at low concentrations. It behaves as a non-flammable and soluble gas. Sulfur dioxide has a relatively low boiling point (about −10 °C, at 1 atm) and a melting point of about −75 °C. It can be easily liquefied at moderate pressure. Table 1 illustrates important physical properties of sulfur dioxide [1].

Table 1- Sulfur dioxide physical properties

Molecular mass	64.06
Melting point (101.3 kPa)	−75.5 °C
Latent heat of fusion (at *mp*)	115.6 J/g
Dynamic viscosity at 0 °C	368 Pas
Density at − 10 °C	1.46 g/cm^3
Critical density	0.525 g/cm^3
Critical pressure	78.8 bar
Critical temperature	157.5 °C
Boiling point (101.3 kPa)	−10.0 °C
Latent heat of vaporization (at *bp*)	402 J/g
Standard density at 0 °C (101.3 kPa)	2.93 kg/m^3
Density relative to air (0 °C, 101.3 kPa)	2.263
Molar volume (0 °C, 101.3 kPa)	21.9 L/mol
Standard enthalpy of formation	−4636 J/g
Specific heat capacity c_p (101.3 kPa):	
0 °C	586 J kg^{-1} K^{-1}
100 °C	662 J kg^{-1}K^{-1}
300 °C	754 J kg^{-1}K^{-1}
500 °C	816 J kg^{-1}K^{-1}
c_p/c_v (15 °C, 1013 mb)	1.29

One of the most significant physical characteristics of sulfur dioxide is its high solubility in water and certain polar solvents The solubility of SO_2 in water is proportional to the partial pressure of SO_2 and follows the behavior of Henry's law and increases as the temperature decreases as shown in Figure 1 [1].

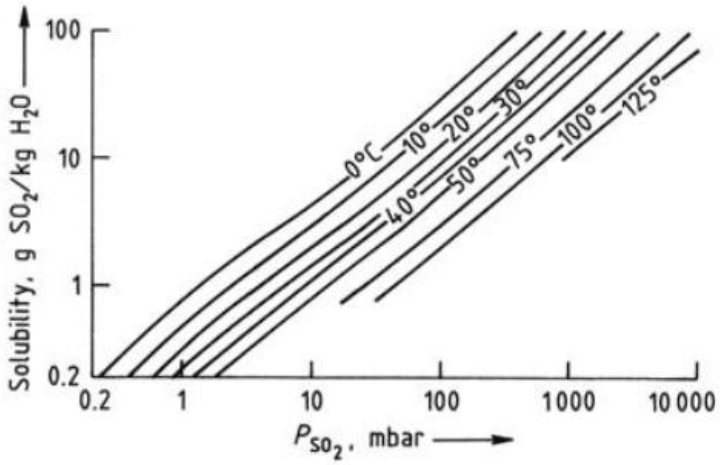

Figure 1- Solubility of sulfur dioxide in water

Sulfur dioxide is fairly stable over a wide range of temperatures and does not start to dissociate appreciably until about 2000 °C. This stability results in extensive use of SO_2 as an intermediate species in sulfur recovery and sulfuric acid plants. Under extreme conditions, such as intense radiation or electrical discharge, significant SO_2 decomposition is only possible [1].

One of the most important reactions related to sulfur dioxide is its oxidation to sulfur trioxide which is the basis of the sulfuric acid production. In the gas phase, the oxidation reaction is written as equation (1.1).

$$2SO_2 + O_2 \rightleftharpoons 2SO_3 \quad (1.1)$$

1.2. Sulfur dioxide production from elemental sulfur

Industrial production of sulfur oxides is commonly based on elemental sulfur combustion because the process is relatively simple to operate and gives high conversion efficiency. Sulfur is introduced into a combustion furnace and reacts with oxygen, generally supplied by air, to produce sulfur dioxide by the exothermic reaction presented in equation (1.2) [1]:

$$S_{(l)} + O_{2\,(g)} \rightarrow SO_{2\,(g)} \quad (1.2)$$

$$\Delta H = -297 \text{ kJ/mol} \quad (1.3)$$

The reaction releases a considerable amount of heat, making the sulfur furnace the main thermal source within the plant. The high heat of reaction is particularly important. The hot process gas is then routed through several exchangers for steam generation and heat recovery.

During oxidation in a vapour phase, the main sulfur species that actually goes into oxidation in combustion is diatomic sulfur (S_2). The evaporation of liquid sulfur initially gives mainly S_8 molecules, which only decompose appreciably to S_2 above about 600 °C. More than 60% of the total heat of reaction, a significant amount of the heat released during combustion, is theoretically used for preheating the incoming air and sulfur feed,

and for the evaporation and decomposition of sulfur. Such results indicate the importance of an efficient heat transfer, especially in the first phase of combustion [1].

The minimum ignition temperature for solid sulfur reaction with the air at 1 atm is 246 °C. However, clouds of sulfur dust can ignite spontaneously at temperatures as low as 190 °C, an important safety consideration in the storage and handling of sulfur. The application of pure oxygen or oxygen-enriched air for sulfur combustion is generally not considered to be economically attractive because of the cost of oxygen supply. Hence, this approach is not widely used in an industrial scale.

The upper practically feasible concentration limit of sulfur dioxide production from liquid sulfur combustion with air is about 18 vol% SO_2. More often, sulfur combustion furnaces associated with sulfuric acid plants produce gases containing 10-12 vol% SO_2, corresponding to an O_2/SO_2 ratio of about 1:1 as normally required in double absorption processes in sulfuric acid production plants [1].

The process air is usually dried with concentrated sulfuric acid before entering the combustion boiler. The dried air is compressed by a blower to a pressure of about 1.3–1.5 bar in order to provide the pressure to overcome the pressure losses downstream. The drying and compression phases normally increase the temperature of the air to about 60-100 °C [1]. Figure 2 represents the theoretical sulfur combustion temperature with respect to SO_2 concentration, considering air and sulfur temperatures of 80 °C and 140 °C, respectively.

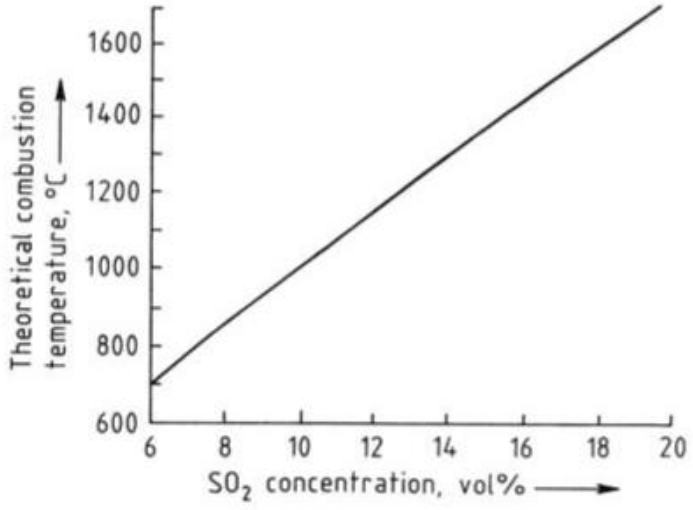

Figure 2- Theoretical sulfur combustion temperatures vs. SO_2 concentration

The combustion temperature is strongly affected by the SO_2 concentration in the outlet gas stream. When liquid sulfur at 140 °C is burned in dried air initially at 60–80 °C, the combustion temperature is typically around 1000 °C for a gas containing 10 vol% SO_2. The combustion temperature increases linearly with respect to the SO_2 purity in the furnace outlet stream, reaching 1600 °C at 18 vol% SO_2 [1].

1.3. Formation of SO_3 and sulfuric acid and associated corrosion risks

The primary reaction in the sulfur furnace is the combustion of liquid sulfur to sulfur dioxide:

$$S + O_2 \rightarrow SO_2 \quad (1.4)$$

$$\Delta H^\circ = -296.8 \text{ kJ/mol} \quad (1.5)$$

The reaction takes place at atmospheric pressure and generates high temperatures in the combustion zone, usually in the range of 1000–1400 °C. Under these conditions sulfur dioxide is the main product and the formation of sulfur trioxide (SO_3) is thermodynamically limited [1] [7]. A second reaction may occur, oxidation of sulfur dioxide:

$$2SO_2 + O_2 \rightleftharpoons 2SO_3 \quad (1.6)$$

$$\Delta H^\circ = -197.8 \text{ kJ/mol} \quad (1.7)$$

This reaction is exothermic, as it produces heat. At high temperatures (above 900 °C) the equilibrium favors the formation of SO_2 so that little SO_3 is formed. As the gas cools, the equilibrium shifts towards the formation of SO_3. At the same time, the reaction rate drops at lower temperatures. Thus, the maximum formation of SO_3 is generally found at an intermediate temperature range. The experimental studies suggest that this range is around 900-1000 °C under homogeneous conditions. In practical systems, the catalytic surfaces may promote the significant SO_3 formation to lower temperatures, often around 600-750 °C [1], [8], [9].

In industrial operation, combustion is carried out with excess air to ensure complete conversion of sulfur. While this is necessary to avoid unburned sulfur, the presence of additional oxygen promotes the oxidation of SO_2 to SO_3 in the post-combustion region. Consequently, even in non-catalytic sulfur furnaces, small amounts of SO_3 are typically present in the outlet gas [1], [8].

The formation of sulfuric acid is directly linked to the presence of SO_3 and water vapor in the air. Sulfur trioxide reacts rapidly with water according to the reaction in equation (1.8).

$$SO_3 + H_2O \rightarrow H_2SO_4 \quad (1.8)$$

$$\Delta H^\circ \approx -130 \text{ kJ/mol} \quad (1.9)$$

This reaction is highly unfavorable and proceeds almost instantaneously when water vapor is present. Since atmospheric air always contains a certain amount of humidity, water is inevitably introduced into the furnace, making the formation of sulfuric acid difficult to avoid when SO_3 is present [7], [8].

As the temperature reaches the sulfuric acid dew point temperature, condensation occurs and may cause corrosion in the equipment. Sulfuric acid dew point temperature depends on the partial pressures of SO_3 and water vapor. Under typical industrial conditions, the acid dew point lies in the range of 120–200 °C, but it can increase beyond 200 °C when SO_3 concentrations are higher [7], [8].

1.4. Sulfuric acid dew point in combustion gases

In combustion systems, the dew point temperature is defined as the temperature at a given pressure at which a gas mixture becomes saturated and condensation begins. Therefore, empirical correlations can be used to connect temperature to the partial pressures of sulfur trioxide and water vapor. One common type of these correlations, first suggested by Verhoff [10], and later improved by Pierce, is shown in equation (1.10) [11].

$$\frac{1000}{T} = 1.7842 + 0.0269\log(p_{H_2O}) - 0.1029\log(p_{SO_3}) + 0.0329\log(p_{H_2O})\log(p_{SO_3}) \quad (1.10)$$

The same relationship can be written using natural logarithms as it is indicated in equation (1.11) [11]:

$$\frac{1000}{T} = 2.276 + 0.02943\ln(p_{H_2O}) - 0.0858\ln(p_{SO_3}) + 0.0062\ln(p_{H_2O})\ln(p_{SO_3}) \quad (1.11)$$

where T is the acid dew point temperature in Kelvin, and p_{H_2O} and p_{SO_3} are the partial pressures of water vapor and sulfur trioxide in mmHg, respectively [11].

These expressions clearly show that the dew point increases with increasing partial pressure of water vapor and sulfur trioxide concentration. As a result, even minor variations in SO_3 content can shift the condensation temperature into the operating range of the heat recovery equipment.

This is an important behavior from the operational point of view. In the course of cooling, the bulk gas temperature alone is not sufficient. The local surface temperatures (e.g., heat exchanger, boiler tubes) may be below the acid dew point, even though the gas temperature is above it. For this reason, controlling SO_3 formation by limiting excessive Oxygen, limiting moisture content by setting a dryer in the inlet air stream, and maintaining adequate temperature limits are essential design considerations in sulfur-based combustion processes [11].

2. Production technologies for sulfur dioxide production

Sulfur dioxide can be obtained from several types of sulfur-containing materials. The feed of these processes can contain elemental sulfur, pyrite, gold-bearing ores, copper sulfide

ores, nickel sulfide ores, zinc sulfide ores, lead sulfide ores, waste sulfuric acid, calcium sulfate, iron sulfate, hydrogen sulfide, flue gas and sulfur trioxide. In modern plants, elemental sulfur is the most commonly used source. When it is burned with air, it produces a gas stream that is relatively suitable for further processing, especially in sulfuric acid production [1], [7].

In other processes, sulfur dioxide is produced in nonferrous metallurgy processes, where materials such as copper or zinc ores are roasted or smelted. The produced gas from these processes contains less SO_2 and often includes dust and other components, which must be removed before the gas can be used. As a result, these processes are normally coupled with gas cleaning processes [1], [12].

Thus, the technology selected is closely linked to the feed material and the overall purpose of the plant. The design of the furnace or reactor and the need for downstream treatment can be influenced by differences in gas composition, temperature level and impurity content. The main production technologies are summarized in Table 2 [1].

Table 2- Sulfur dioxide technologies

No.	Sulfur source/feed	Technology/ furnace type	Main reaction(s)	Typical operating conditions	Short description / main features
1	Elemental sulfur (liquid sulfur)	Liquid sulfur combustion furnace [1]	$S+O_2 \rightarrow SO_2$	Air is dried and compressed to 1.3–1.5 bar, reaching to the temperature range of 60–100 °C. Liquid sulfur is fed at 140–150 °C to reduce viscosity and improve atomization. Under these conditions, combustion gas contains about 10–12 vol% SO_2 ($SO_2/O_2 \approx 1:1$). In industrial operation, SO_2 concentration can reach ~18 vol%. Theoretical combustion with sulfur temperature of 140 °C and air temperature range between 60–80 °C gives approximately 1000 °C furnace temperature and the purity of 10 vol% SO_2, while increasing the temperature to ~1600 °C raises SO_2 concentration to ~18 vol%, indicating a linear relationship [1].	This is the standard modern route for SO_2 production from elemental sulfur, where sulfur is atomized into fine droplets to enhance evaporation and improve mixing with air. A waste-heat boiler is installed to recover heat for steam generation and to cool the process gas [1].
2	Elemental sulfur (liquid sulfur)	Pressure-nozzle burner furnace [1]	$S+O_2 \rightarrow SO_2$	Liquid sulfur is fed at a pressure of 8–15 bar, with a maximum throughput per burner of 72 t/d [1].	A simple atomization system using a single spray head is used in many plants; however, operational flexibility is limited, as significant turndown changes generally require nozzle replacement, and smaller nozzles are more susceptible to clogging [1].

3	Elemental sulfur (liquid sulfur)	Two-component burner furnace [1]	$S+O_2 \rightarrow SO_2$	Used mainly for very low sulfur throughputs (< 7 t/d), with sulfur pressure of about 2 bar. Modern plants are designed for capacities up to approximately 170 t/d per burner, with a typical turndown limit of around 15% of capacity; in compact designs, such as those used in pulp mills, operation can be reduced to about 5% of the nominal capacity of 5 t/d [1].	Sulfur atomization in this design is achieved using combustion air instead of depending only on sulfur pressure, which makes this arrangement more suitable for low-capacity applications where pressure-nozzle burners are not practical. [1].
4	Elemental sulfur (liquid sulfur)	Rotary burner sulfur furnace (Lurgi/LURO burner) [1]	$S+O_2 \rightarrow SO_2$	Sulfur is fed into the furnace at atmospheric pressure and flows through a rotating element at 4000–6000 rpm. This configuration is applicable for capacities in the range of 5–400 t/d [1].	This type of burner is used in large sulfur-burning plants, where the sulfur is first distributed centrifugally in a rotating cup and then atomized by primary air. Most of the combustion air is provided by secondary air and an adjustable air system creates a tangential flow pattern to stabilize the flame and minimize droplet impingement on the furnace walls. [1].
5	Elemental sulfur (liquid sulfur)	Two-stage sulfur combustion process	Stage 1: sulfur combustion. Stage 2: oxidation of remaining sulfur vapor with added air [13]	The first stage is operated in an oxygen-deficient atmosphere at about 1750 °C. The result is combustion and unconverted sulfur vapor in the gas. Gas is cooled with a waste heat boiler to 620–650 °C before entering the second stage. The final gas has a concentration of about 18 vol% SO_2 and after passing through the after-	This process was developed for high SO_2 concentrations with minimization of NO_x formation. The high SO_2 content (~18 vol%) limits the availability of free oxygen and reduces the formation of NO_x [1] [14].

				burner leaves at a temperature not exceeding about 700 °C and enters the waste heat boiler (steam superheater generator) and then goes to a liquefaction or bisulfite plant [1].	
6	Pyrite concentrate	Roasting of Pyrites occurs in a flotation mode	Overall roasting reaction represented by [14]: $2FeS_2 + 5.5O_2 \rightarrow Fe_2O_3 + 4SO_2$	Ignition occurs in the range of 350 to 550 °C, while complete reaction is only assured at temperatures above 800 °C. The optimum operating range is usually between 850 and 940 °C, depending on particle size. In the case of air, the SO_2 concentration in the roaster gas could be as high as ∼16 vol% under favorable conditions, but 13–14 vol% is more typical due to excess air [1].	The technology is widely preferred in the modern pyrite roasting due to its better temperature control, higher processing capacity and more favorable economic performance compared to the old roasting systems [1].
7	Pyrite concentrate	Dorr-Oliver fluo solids reactor (wet feeding principle) [15]	Overall roasting reaction represented by: $2FeS_2 + 5.5O_2 \rightarrow Fe_2O_3 + 4SO_2$	The bed is generally operated at temperatures between 600 and 900 °C, with gas velocities maintained in the range of 0.2–0.6 m/s, and a specific throughput of approximately 4–5 t per square meter of roaster area per day [1].	The fluidized-bed design operates on a wet feeding principle, where floating pyrites are combined with water to form a sludge containing approximately 70–80% solids [1].
8	Pyrite concentrate	BASF–Lurgi fluid-bed furnace	Overall roasting reaction represented by: $2FeS_2 + 5.5O_2 \rightarrow Fe_2O_3 + 4SO_2$	The bed is typically operated at temperatures of 650–900 °C, while the gas space above the bed may reach up to 950 °C. The system is maintained at a slightly sub-atmospheric pressure to prevent sulfur leakage to the surroundings. The roaster outlet gas is 350 °C with an SO_2 concentration of 14–14.5 vol%. The design capacity for pyrite throughput is about 1000 t/d [1].	This design is intended to maximize heat recovery and generate high-pressure steam. Indirect cooling through immersed heat exchange elements is used to maintain bed temperatures to reduce the risk of sulfur trioxide formation. In this process, the oxidation of SO_2 to SO_3 is

					limited by reducing excess oxygen and rapidly cooling the gas stream [1].
9	Gold-bearing ores / special sulfide ores	Circulating fluid-bed (CFB) roasting (Lurgi technology) [1]	This process is based on the calcination of alumina or clay with the combustion of coal to produce a calcined solid and a gas rich in SO_2 [1].	Gas velocities are in the range of 3-6 m/s, roasting is carried out using air or oxygen-enriched air, and the system is designed to promote strong circulation of solids [1].	The design improves the heat and mass transfer compared to conventional stationary fluidized beds and the roasting conditions can be optimized by changing the oxygen partial pressure [1].
10	Pyrite/flotation pyrite	Cyclone furnace roasting	Roasting/oxidation of pyrite with partial melting of solids and recovery of nonferrous metals [1].	The air is preheated in this process for combustion [1].	It is a pilot-scale approach in which the particles melt and flow along the cyclone wall, while the exiting gas stream carries dust along with entrained iron oxide and other mineral compounds. [1].
11	Arsenical pyrite	Boliden process	$2\mathrm{FeAsS} + 5\mathrm{O}_2 \rightarrow \mathrm{Fe}_2\mathrm{O}_3 + 2\mathrm{SO}_2 + As_2\mathrm{O}_3$	In the Boliden process, magnetite is formed at 850 °C in the first stage, followed by sulfur vapor combustion in a separate chamber during the second stage, with high-pressure steam generated at around 425 °C per tonne of pyrites. [16].	Plants with capacities of around 500 t/d are operated in many countries under Lurgi license [1] [17].
12	Arsenical pyrite	Two-stage roasting (BASF process) [17]	$\mathrm{FeS}_2 + \mathrm{O}_2 \rightarrow \mathrm{Fe} + \mathrm{SO}_2$	In the first step the process is operated at approximately 900 °C. In the second step Fe_2S is roasted at approximately 800 °C and the outlet gas leaving the cyclone has a concentration of about 18 vol% SO_2 [1].	The outlet gas temperature is reduced by a waste heat boiler system [1].

13	Copper sulfide ores ($CuFeS_2$, etc.)	Reverberatory furnace smelting [18]	Overall oxidation of sulfides → SO_2	The concentration of SO_2 in the off-gas stream is about 1–2 vol%, which results in higher fuel consumption and makes the process less suitable for sulfuric acid production [1].	This process generates a dilute SO_2 gas and is considered not feasible because of its high energy consumption [1].
14	Copper sulfide ores	Electric furnace smelting [1]	Overall oxidation of sulfides → SO_2	In this method, the SO_2 concentration typically ranges between 3 and 10 vol% [1].	This method is typically applied where low-cost electricity is available, and carbon dioxide and carbon monoxide are formed as a result of electrode oxidation [1].
15	Copper sulfide ores	Flash smelting furnace (Outokumpu process) [19]	$Cu_2S + O_2 \rightarrow Cu + SO_2$	The smelting furnace operates with an outlet temperature of approximately 1200–1300 °C, using oxygen-enriched air containing 45–60% O_2. The waste gas produced contains about 10–13 vol% SO_2, along with approximately 1 vol% O_2 and 0.05 vol% SO_3, with a gas volume of around 6000–6500 m^3 per tonne of copper. The inlet air is preheated to temperatures in the range of 450–750 °C [1].	In this process, oxygen-rich air is fed to the furnace [1].
16	Copper sulfide ores	Inco flash smelting process	Overall oxidation of sulfides → SO_2. Same principle as flash smelting	The process operates with a throughput of up to 1500 t/d, utilizing a fluidized-bed pretreatment dryer and approximately 95% oxygen; the off-gas flow rate is about 1090 m^3 per tonne of copper and contains around 80 vol% SO_2, which is subsequently converted to liquid SO_2 [1].	This is an oxygen-rich process characterized by high efficiency and a compact design [1].

17	Copper sulfide ores	Flame cyclone furnace, combined with the electric resistance process, which is used in the Kivcet process [20]	A cyclone is used to oxidize the sulfides. The feed contains zinc, lead, and copper. [1].	The off-gas leaving the furnace at 1250–1350 °C, and SO_2 concentration is 80–85 vol% [1].	This is a high-intensity smelting process combining a cyclone reactor and an electric furnace, with high SO_2 concentrations and gas volumes in the range of 800–2000 m^3 per tonne of copper produced [1].
18	Copper smelting of sulfide ores	Converter (Mitsubishi process)	Oxidation of Copper matte → SO_2	The amount of SO_2 in off-gas streams may vary significantly. The Mitsubishi process has minimized these variations [21].	The gas composition varies significantly. Separate process stages were connected by laundars to keep the concentration stable [22] [1].
19	Nickel smelting, nickel sulfide ores, pentlandite $(Ni, Fe)_9S_8$, pyrrhotite (Fe_7S_8), chalcopyrite ($CuFS_2$) [1]	Fluid-bed roasting furnace/flash smelting [1]	$3Fe_7S_8+38O_2 \rightarrow 7\ Fe_3O_4 + 24SO_2$	In fluidized-bed furnaces, operation typically occurs at around 650 °C, where an air flow of approximately 40,000 m^3/h results in SO_2 concentrations close to 12 vol%. In the Outokumpu flash smelting process, similar SO_2 levels of about 10–12 vol% are obtained when using preheated roasting air at 500 °C. By increasing the oxygen content to 27–35 vol%, the nickel throughput can be raised from 400 to 700 t/d, which leads to an increase in SO_2 concentration in the off-gas to approximately 17–18 vol% [19]. In comparison, the Inco smelting furnace allows much higher throughputs, up to 1500 t/d of nickel, producing off-gas streams with SO_2	This process is similar to copper smelting and blowing. The concentration of SO_2 can be increased by adding more oxygen or using different furnace designs [1].

				concentrations of around 80 vol%, which are then recovered as liquid sulfur dioxide. This process is typically operated at an annual capacity of about 110,000 t/year [1].	
20	Zinc sulfide ores (ZnS)	Fluid-bed roasting process (Vieille Montagne–Lurgi) [23]	$2ZnS+3O_2 \rightarrow 2ZnO+2SO_2$	The roasting operation is operated at 900–1000 °C. The produced gas contains 9–11 vol% SO_2 and 5–6 vol% excessive oxygen [1].	This process is widely applied because of its stable operation and effective heat recovery. The inlet feed contains 8% moisture. For every tonne of concentrate processed, 1 tonne of high-pressure steam at 400 °C is generated [1].
21	Zinc sulfide ores	Sanki–Dorr process (wet feed fluid bed) [1]	$2ZnS+3O_2 \rightarrow 2ZnO+2SO_2$	The roasting process operating temperature is 930 °C [1]	This process generates 0.68 t per tonne of concentrate, which is lower than other processes. This process produces ten times more dilute scrubber acid, which is considered as waste. The slurry, which is fed to the furnace, contains 78% solids [1].
22	Lead sulfide ores (PbS) with 60% Pb and 17% S content	Sintering / Imperial smelting shaft furnace to recover Zn and Pb at the same time [24] [25]	Multi-step oxidation forming PbO + SO_2	Oxygen is absorbed on the particle surface. Lead sulfate is formed, which reacts with additional lead sulfates and oxygen to produce sulfates and litharge (PbO). Ultimately, sulfur dioxide with a concentration of 4–6 vol% is produced [1].	The SO_2 concentration is 5 to 7 vol%. Sulfur trioxide is formed due to the presence of iron oxides. The concentration of sulfur trioxide is 5–10% and it is relative to the SO_2 content. [1].

23	Lead sulfide ores	QSL process (Queneau–Schuhmann–Lurgi) [1]	$2PbS+2.5O_2 \rightarrow Pb+PbO+2SO_2$	The outlet gas leaves the furnace at a temperature of 1200 °C and contains 15–20 vol% of sulfur dioxide [1].	The production capacity of lead is 60,000–75,000 t/a, and has a high concentration of sulfur dioxide [1].
24	Waste sulfuric acid processing	Thermal decomposition furnace	$H_2SO_4 \rightarrow SO_2 +H_2O+0.5O_2$	The decomposition occurs at 1000 °C. The process is endothermic, and indirect heating is applied. The energy consumption is 6.4×10^6 kJ per tonne of H_2SO_4 [26].	This process is applied for acid regeneration and requires an external energy for decomposition and to evaporate the water [1].
25	Waste sulfuric acid processing	Lurgi decomposition furnace (atomizing viscous spent sulfuric acid) [26]	$H_2SO_4 \rightarrow SO_2+H_2O+O_2$	The decomposition of sulfuric acid requires a temperature of 1000 °C. The combustion gases flow into the furnace at 1800 °C. The produced SO_2 gas is cooled to 350 °C with an energy recovery system. [1].	The pressure of the inlet air is 1.35 bar. The air excess amount is 10-30% to ensure combustion. The furnace temperature is adjusted by the inlet air flow rate. [1].
26	Waste sulfuric acid processing	Grillo rotary kiln process using a stationary fluid bed system [1]	Multi-stage decomposition process following a downstream combustion chamber and two post-combustion chambers [1].	The operating temperature range of the rotary kiln process is between 900 and 1000 °C [1].	The process is relatively easy to control [1].
27	Waste sulfuric acid processing	Process developed by Hechenbleickner is also considered as reductive decomposition [27]	Decomposition of sulfuric acid → SO_2	In this process, sulfuric acid is mixed with tar sludge or coal, which lowers the decomposition temperature to the range of 200–600 °C. As a result of the reduction process, sulfur dioxide and coke are produced [1].	This process is effective for a wide range of mixed feeds containing approximately 0.5–60 wt% carbon and 40–90% sulfuric acid. This process is commonly applied in oil refineries, where sulfuric acid is combined with lubricating oils [28] [1].

28	Calcium sulfate (gypsum)	Müller–Kühne process, decomposition in a rotary kiln [29]	$4CaSO_4 + 2C \rightarrow 4CaO + 4SO_2 + 2CO_2$	Calcium sulfate decomposes at temperatures of 900–1400 °C, producing sulfur dioxide–containing gases along with cement clinker. This product can be utilized to produce Portland cement [1].	The process produces sulfur dioxide along with cement clinker and is characterized by high energy consumption [1].
29	Iron (II) sulfate (in heptahydrate form, which is called green salt)	Thermal decomposition using fluid bed furnaces, multiple hearth furnaces, and rotary kilns [30]	Iron sulfate with 7 waters $\rightarrow Fe_2O_3 + SO_2$	Dehydration is performed in the first stage in fluidized-bed dryers at 130–200 °C. The second stage is the decomposition of sesquihydrates at 900 °C [1].	In previous technologies, decomposition was performed in sintering machines or rotary kilns, producing gas streams with 7 vol% SO_2. In more recent technologies, fluidized-bed pyrite roasters operate at 850 °C. The off-gas leaves the furnace at 350–400 °C before entering the gas cleaning stage [1].
30	Hydrogen sulfide (H_2S) (high concentration from natural gas purification plants, oil refinery plants, liquefaction and gasification plants)	The Claus process converts H_2S to elemental sulfur and produces an off-gas stream that can be burnt to form sulfur dioxide. This product can then be further processed to produce sulfuric acid in wet acid plants. [1].	$2H_2S + 3O_2 \rightarrow 2SO_2 + 2H_2O$	The combustion temperature is usually between 500 and 1000 °C, depending on the sulfur concentration in the stream [1].	This method is applied to waste gas streams where the concentrations of sulfur oxides can be as high as 10 vol % or more [1].

31	Hydrogen sulfide (low concentration)	Catalytic incineration [1]	$2H_2S + 3O_2 \rightarrow 2SO_2 + 2H_2O$	The presence of a catalyst enables the process to be carried out at relatively low temperatures (usually about 200 °C [1].	This process does not require additional fuel and is used when thermal combustion is not efficient due to a low concentration of hydrogen sulfide, which results in a higher SO_2 concentration in the produced gas [1].
32	Flue gases (low SO_2 content)	BF regenerative adsorption process [1]	SO_2 adsorption → thermal regeneration	This method is a dry flue gas treatment process in which sulfur dioxide is captured by adsorption on activated carbon at around 130 °C with the efficiency of 80–95%. The retained SO_2 is then oxidized in the presence of moisture to form sulfuric acid. During regeneration at 600–650 °C, this acid decomposes to sulfur trioxide, which is subsequently reduced by coke back to sulfur dioxide in the final stage [1].	This method is used to dilute SO_2 streams. The regeneration occurs in a moving-bed reactor, and the concentration of sulfur dioxide is raised to 25 vol % [1].
33	Chemical production from sulfur trioxide and sulfur	Exothermic reaction by IG Farbenindustrie [1]	$S+2SO_3 \rightarrow 3SO_2$	Solid sulfur is fed to the reactor at 110 °C, and an oleum stream containing 26–30% SO_3 is fed in from the bottom. After the reaction, about 5–10 vol% SO_3 is present in the outlet gas, which is scrubbed with sulfuric acid to improve the purity of the sulfur dioxide [1].	The start-up process requires an external heat input. The main advantages of this method are low capital cost and operational simplicity. The production of 1 tonne of liquid sulfur dioxide normally demands about 20 kWh of electrical energy and 30 m^3 of water at 20 °C [1].

There is a clear tendency when looking at these technologies. Processes using the combustion of elemental sulfur and oxygen-enriched smelting produce high SO_2 concentrations, and they are ideal for the production of sulfuric acid. Older technologies, such as reverberatory furnaces or sintering processes, on the other hand, lead to much more dilute gas streams, making recovery more difficult and less economical.

Another important observation is that modern processes are increasingly designed with heat recovery and gas conditioning in mind. Almost all high-temperature processes are directly coupled with waste heat boilers, and many include gas cleaning and concentration steps to make the SO_2 stream suitable for further processing [1].

The next stage in the process is the cleaning stage, as the sulfur dioxide stream can contain a variety of other impurities. The most common impurities can be considered as [1]:

- Primary dust (from roasting or metallurgical extraction processes)
- Fumes (substances which resolidify in the form of aerosol, such as zinc, lead, zinc oxide, lead sulfates, etc.)
- Volatiles (substances in the form of a gaseous state which can be precipitated in the dedusting systems, such as arsenic, selenium, mercury, sulfuric acid mists, and hydrocarbons)
- Gaseous substances (substances such as hydrogen chloride, hydrogen fluoride, carbon dioxide, carbon monoxide, lower hydrocarbons)

The main gas cleaning technologies and the recovery and purification technologies are summarized in Tables 3 and 4 [1].

Table 3- Sulfur dioxide gas cleaning technologies

No.	Sulfur source/feed	Technology/ system	Main reaction(s) and mechanism	Typical operating conditions	Short description / main features
1	Roaster/smelter gases (dusty SO_2 gas)/ waste gases	Cyclone separator (dry dedusting) [1]	Mechanical separation of coarse particles, electrostatic precipitation, and separation	The furnace waste gas is directed to a separation cyclone, where a pressure drop of 5–10 mbar occurs, and 85–90% of the dust is removed. The remaining impurities are eliminated using an electrostatic precipitator. [1].	The electrode discharge voltage typically ranges from 10 to 80 kV. The specific power consumption for the process is about 1–2.5 kWh per 1000 m^3 of gas [1].
2	SO_2 gas with volatile impurities	Venturi scrubber / wet scrubbing tower [1]	Gas–liquid contact → absorption & condensation	The gas is cooled to 60–80 °C using an adiabatic water evaporation system. This system also removes impurities such as selenium, arsenic trioxide, and sulfuric acid. The additional contaminants are removed by a wet electrostatic precipitator. In addition, settling tanks may be used for the separation of solid particles [31] [1].	Fresh water is recirculated for the removal of volatile impurities such as arsenic, selenium and acid mist, and to cool the gas before it enters the acid plant. A fluorine removal tower may be employed to remove hydrofluoric acid. In this tower, silica packing reacts with hydrogen fluoride to form fluosilicic acid [1].
3	SO_2 gas streams with Mercury (Hg)	Mercury removal (dry/wet methods) [32]	Adsorption or chemical conversion	This process is often integrated with the gas cleaning system. In the dry method, the gas passes through a filtration medium containing selenium, which reacts to form mercury(II) selenide. In the wet method, elemental selenium is used in a scrubber and the gas is washed with a mercury(II) chloride solution	This process is important for compliance with the environmental regulations and the purity of the produced acid [1].

				to convert mercury into insoluble mercury(I) chloride, which is then removed by sulfuric acid as mercuric sulfate [1].	

Table 4- Sulfur dioxide recovery and purification technologies

No.	Sulfur source/feed	Technology/ system	Main reaction(s) and mechanism	Typical operating conditions	Short description / main features
1	SO_2-rich gas	Partial condensation process [1]	Cooling → liquefaction of SO_2	The condenser is operated at temperatures between −40 and −70°C. Evaporation of the coolant occurs on the shell side. The optimum inlet SO_2 concentration is 16–18 vol %. Under these conditions about 12 vol% SO2 can be condensed and about 6 vol% remains in the residual gas. The energy consumption is estimated to be 260 kWh of electricity and 90 m3 of water at 20 °C per tonne of liquefied sulfur dioxide [1].	his is one of the most common industrial processes for the production of liquid SO2, which has been historically operated by Lurgi. This process is energy-efficient at high SO2 concentrations and under these conditions 30–60% of the incoming sulfur dioxide can be condensed [1].
2	SO_2 gas streams	Bayer process, Gas compression, and condensation	Compression and cooling	Roaster gas containing about 6–7 vol% SO_2 is first compressed to approximately 5 bar and then directed to the cooling section, where ammonia is used as the refrigerant. The temperature is reduced to around −70 °C in a flashing process [1].	For a plant with a capacity of 25–30 t/d, the production of 1 tonne of sulfur dioxide requires an energy consumption of 680 kWh [1].
3	SO_2 gas streams	Absorption with water (Hänisch–Schröder process)	Absorption → desorption	In this process, SO_2 concentration should be more than 10–11 vol% for a stable process. It is done in a packed tower. Water is fed in from the top and flows counter-current to the gas	This is one of the oldest methods, characterised by its relatively simple operation but high energy demand. It takes about 120

				stream absorbing the sulfur dioxide. The liquid leaving contains about 1–2 wt% SO_2 and then goes to a desorption tower at low pressure to separate the dissolved sulfur dioxide from the water [1].	m^3 of water, 3 tonnes of steam and 90 kWh of electrical energy to produce 1 tonne of liquefied sulfur dioxide [1].
4	SO_2 gas streams	Pressurized water absorption (Grillo process) [1]	Absorption under pressure and stripping	Sulfur dioxide gas with a minimum concentration of about 9 vol% is compressed to 5 bar and cooled to 50 °C. It is introduced to an absorption tower where it is washed with water. The enriched liquid is then sent to a desorption column where sulfur dioxide is stripped with low-pressure steam [1].	This method produces liquid SO_2 but consumes a large amount of compression energy. For an inlet gas concentration of about 10 vol % about 300 kWh of electrical energy is needed to produce 1 tonne of liquid sulfur dioxide [1].
5	SO_2 gas streams	Absorption in alkaline solution [1]	Chemical absorption	Depending on the process, different absorbents can be used. For strong bases, caustic soda or ammonia can be considered. For weak organic or inorganic acids absorbents such as sodium carbonate, citrate, aliphatic or aromatic amines can be used [1].	Weak bases are more efficient and require less energy for regeneration than stronger absorbents [1].
6	Flue gas / dilute SO_2	Wellman–Lord process [33]	Reversible absorption with Na_2SO_3/$NaHSO_3$	In the first step, the flue gas is treated by an electrostatic precipitator for the removal of particulate matter and then sent to the absorption unit. The flue gas is scrubbed in a counter-current configuration using sodium sulfide or sodium bisulfite solutions. The regeneration step is carried out by indirect steam heating. [33] [1].	This process generates a concentrated SO_2 stream. It is widely used in flue gas desulfurization systems in power plants, and for treatment of tail gas from Claus sulfur recovery units. [1].

7	Flue gas / dilute SO_2	Amine adsorption process [1]	Adsorption with Amine Solution	Amines have a greater ability to absorb sulfur dioxide than solutions of sodium sulfide [1].	Amine-based absorbents are generally easier to regenerate, but the release of amines can be a health risk [1].
8	Flue gas	Sulfidin process [34]	Adsorbents are Xylidine and Toluidine	This process is considered environmentally harmful [1].	The process has been phased out largely because of the negative environmental effects [1].
9	Tail gas from Claus plants	UCAP process [35]	The absorbent used is the aqueous solution of triethanolamine [1]	The resulting sulfur dioxide is reprocessed and recycled in purified form [1].	It can be used in Claus process plants for additional sulfur recovery [1].
10	SO_2 flue gas streams	Physical absorption process by Linde (Solinox) [36]	Physical absorption with polyethylene glycol dimethyl ether	Sulfur dioxide of 80–90% purity is produced by this process [1].	It is used for the purification and concentration of SO_2-contain gas flows [1].

3. Industrial plant model description

3.1. Process description of sulfur dioxide production unit

This plant is designed to produce sulfur dioxide using liquid sulfur and air as feed streams. The plant operates with a capacity of 6000 kg/h of liquid sulfur. The main equipment is the furnace. The function of the furnace is to carry out the combustion required for Sulfur dioxide generation. In addition, a reboiler is used as the furnace cooling system, referred to as separator-reboiler vessel, surge drum or surge tank. This unit is responsible not only for cooling the furnace but also for generating superheated vapor at elevated temperatures for use in other sections of the plant. In this section, the operating case of the unit is described.

The combustion furnace is the heart of the plant. In this section, sulfur is burnt with ambient air to form sulfur dioxide (SO_2). The oxygen necessary for the reaction is supplied from ambient air. In the boiler, sulfur is injected as fine droplets and ignition occurs upon contact with a flow of hot air in the combustion chamber, releasing a large amount of heat [38].

This thermal energy is recovered in a fired-tube boiler and the circulating water is converted into high-pressure steam. At the same time, heat recovery reduces the outlet gas temperature to a suitable operating level. The gas is subsequently subjected to washing, purification, and drying steps before being filled into cylinders for distribution. Alternatively, the gas can be further processed to produce salts such as sulfite and bisulfite powders [37].

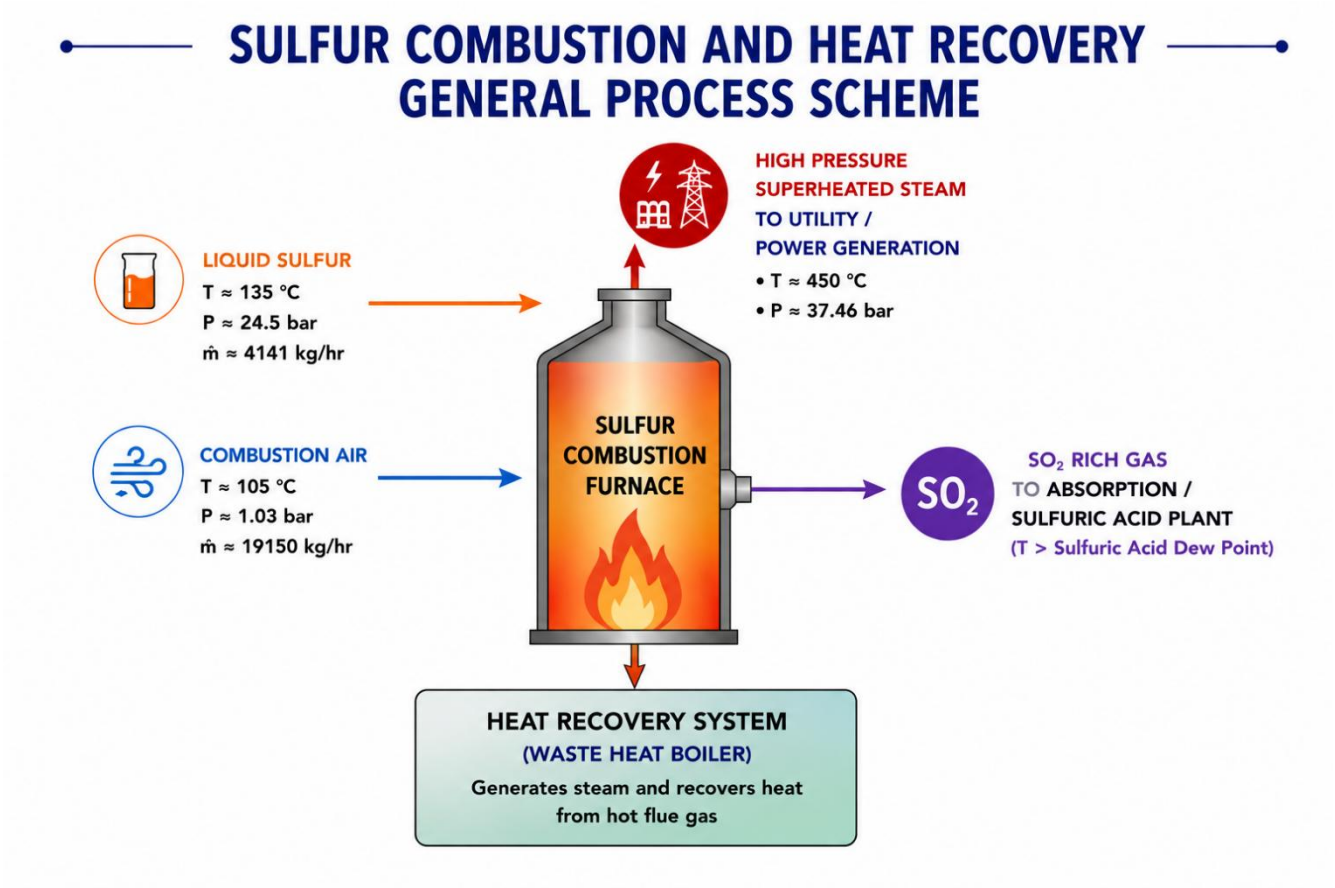

Figure 3-Sulfur combustion and heat recovery process scheme

3.2. Horizontal separator-reboiler

A horizontal separator–reboiler is a process equipment that combines phase separation and heat transfer functions, allowing the separation of vapor–liquid mixtures while simultaneously providing the desired vapor and liquid for different sections of the process. Such equipment is commonly used in thermal systems where both phase equilibrium and controlled vapor production are required [38].

The cooling system fluid for this unit is water in different forms, including liquid, vapor, and two-phase streams. The cooling system is managed by a horizontal separator and reboiler vessel. This equipment separates the two-phase streams to ensure fluids are provided to other parts of the system. In addition to its separation function, this equipment provides sufficient heat to the liquid with a heating coil, enabling the

generation of vapor required for a specific section of the furnace. Therefore, this vessel performs both separation and boiling functions.

The separator operates with a total of seven main process streams, consisting of two inlet streams (including stream 7 referred to the outlet of Evaporator EX-EVAP3 and stream 4 referred to Economizer EX-ECO), three outlet streams (including stream 8 referred to inlet of Superheater EX-SUP1, stream 5 referred to inlet of Evaporator 1 EX-EVAP1 and partial inlet of Economizer EX-ECO, stream 14 referred to inlet of reboiler2), and two streams associated with the inlet and outlet of the heating coil (stream 10 referred to inlet of Superheater EX-SUP2, stream 9 referred to outlet of Superheater EX-SUP1). Since all streams connected to this vessel are directly linked to the furnace, their detailed description is provided in the corresponding furnace section.

3.3. Furnace

A sulfur combustion furnace is a high-temperature process equipment designed to burn sulfur in the presence of air to make sulfur dioxide (SO_2) [1]. Furnace is the main part of the sulfur production unit. The liquid sulfur feed is in the range of 3500-6000 kg/h for productivity reasons, and the value of 4140 kg/h was chosen as the case study. Therefore, the elemental liquid sulfur flows into the furnace at 24.5 bar and 135 °C with a rate of 4140 kg/h. The pressure is decreased to 4.45 bar by a valve before entering the furnace. Then, sulfur is sprayed into the combustion zone and it reacts with oxygen to make sulfur dioxide. Oxygen is supplied from ambient air. The air stream, with a flow rate of 19150 kg/h and at a pressure of 1 bar, is preheated to 105.1 °C using a heat exchanger identified as EX-Air before entering the furnace. The flow rates of air and sulfur indicate a significant excess oxygen relative to the stoichiometric requirement.

The furnace has a non-conventional design, specifically developed for this unit. It is configured as a horizontal furnace consisting of two chambers and six heat exchangers are dedicated to heat recovery which are evaporator 1 (EX-EVAP1), evaporator 2 (EX-EVAP2), superheater 2 (EX-SUP2), superheater 1 (EX-SUP1), evaporator 3 (EX-EVAP3), and the economizer (EX-ECO).

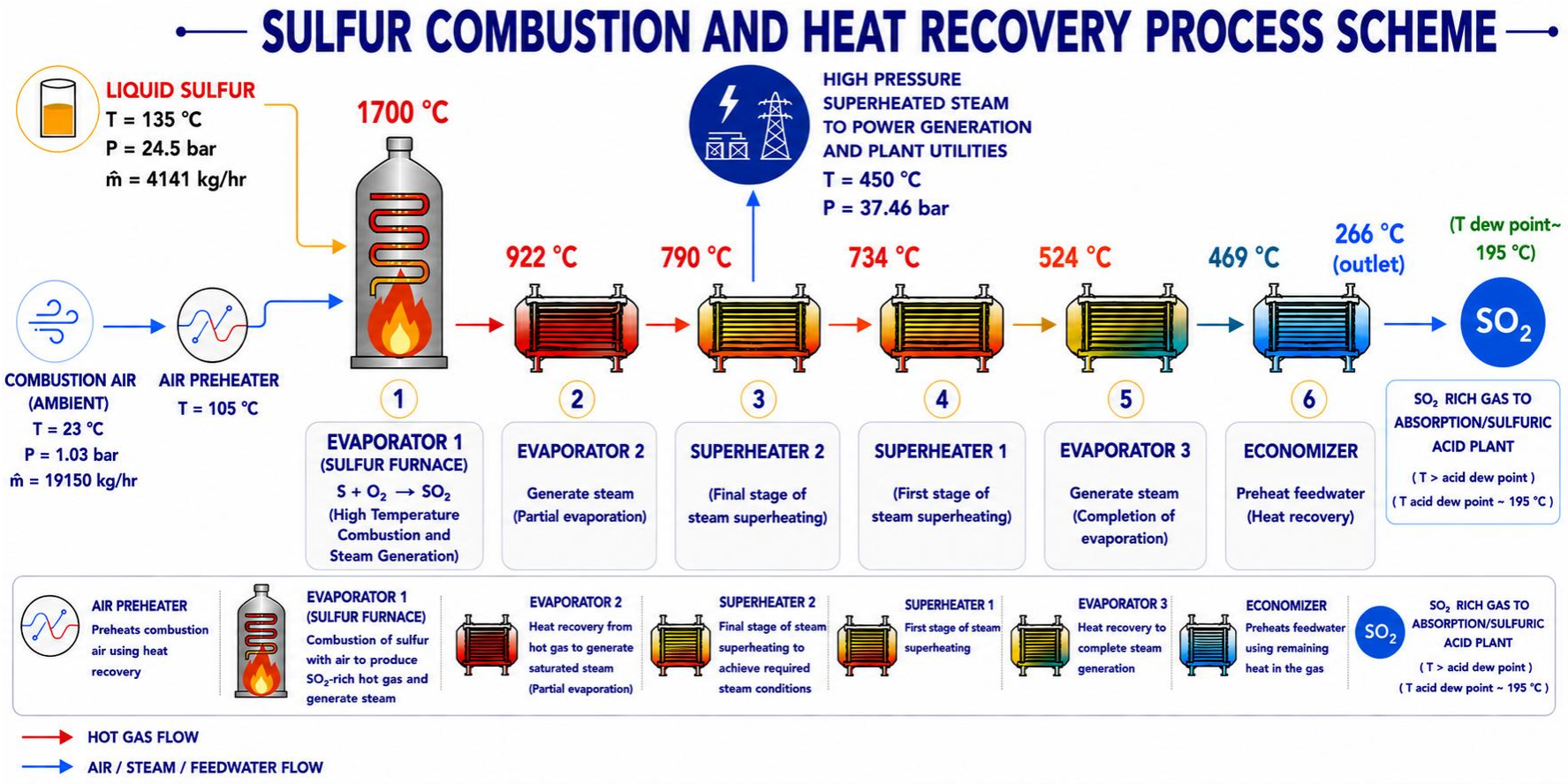

Figure 4-Sulfur combustion and heat recovery process scheme

3.3.1. Stage 1 of heat recovery (evaporator 1 EX-EVAP1)

In the first chamber, the initial stage of the heat transfer system is located, where only evaporator 1 (EX-EVAP1) is installed. Combustion takes place in this section. Liquid sulfur reacts with the inlet air to produce sulfur dioxide at a temperature of approximately 1700 °C. The hot gas is simultaneously cooled by water supplied from the reboiler. At the outlet of this section, the stream reaches a temperature range of 915-925 °C at a pressure of 1 bar, with a total flow rate of 23290 kg/h. The cooling water enters this stage at 248 °C and 42 bar, and a flow rate of 170554 kg/h in the liquid phase. Although the outlet conditions of the cooling stream are not explicitly specified, simulation results indicate that, as heat is transferred, the stream partially vaporizes and enters a two-phase region. Due to frictional effects, a slight pressure drop occurs, reducing the pressure to approximately 40.3 bar, while the vapor fraction increases to about 0.06. The main combustion products in this section are nitrogen, sulfur dioxide, and a certain amount of unreacted oxygen, which remains due to the excess air supplied.

3.3.2. Stage 2 of heat recovery (evaporator 2 EX-EVAP2)

The combustion products then enter the second chamber, where five cooling stages occurs. The first heat exchanger is identified as evaporator 2 (EX-EVAP2). In this heat exchanger, the temperature of the sulfur dioxide stream decreases from the range of 915-925 °C to 785-795 °C. The cooling fluid is being provided from the outlet stream of the first heat transfer stage. This cooling stream enters a two-phase region and, as it flows through the exchanger, experiences an additional pressure drop and the pressure reaches to 39.3 bar, and the vapor fraction increases to 0.08.

3.3.3. Stage 3 of heat recovery (superheater 2 EX-SUP2)

The third heat transfer stage corresponds to superheater 2 (EX-SUP2), where the sulfur dioxide stream is further cooled from the temperature range of 785-795 °C to 730-740

°C. The cooling stream of this stage is provided from the outlet of the coil system in the separator-reboiler. This stream leaves the heating coil system in the vapor phase at 318 °C, 37.5 bar, and a flow rate of 8362 kg/h. It is then combined with an auxiliary stream coming from the outlet of the fourth heat exchanger. This mixing is controlled by a temperature control valve, associated with controller, to regulate the temperature and provide additional heating to the stream. This stream leaves the furnace as a superheated vapor condition at 450 °C and 37.5 bar. This superheated stream is directed to the power generation turbines.

3.3.4. Stage 4 of heat recovery (superheater 1 EX-SUP1)

Superheater 1 (EX-SUP1) is the fourth heat exchanger in the furnace. The temperature of the main sulfur dioxide stream decreases from the temperature range of 730-740 °C to 520-530 °C in this heat exchanger. The cooling stream is supplied from the vapor outlet of the reboiler vessel. It enters at 248 °C, 38.32 bar, and a flow rate of 15920 kg/h. This stream leaves as superheated vapor at the temperature range of 540-550 °C and 38.3 bar from the outlet of this heat exchange. A portion of this stream is then sent through a valve to heat up the inlet stream of superheater 2 (EX-SUP2). This stream finally flows to the reboiler as the inlet heat coil stream.

3.3.5. Stage 5 of heat recovery (evaporator 3 EX-EVAP3)

The fifth heat exchanger is evaporator 3 (EX-EVAP3). The sulfur dioxide stream temperature decreases from the temperature range of 520-530 °C to 465-475 °C in this heat exchanger. The cooling fluid is provided from the second heat exchanger's outlet stream, evaporator 2 (EX-EVAP2). The exact conditions of this cooling stream aren't given, but simulations show that it comes in at about 248 °C, 39.3 bar, and 0.08 vapor fraction. The pressure of this stream drops slightly and reaches 38.3 bar, and the vapor fraction rises to 0.09. After this step, the stream flows back to the reboiler.

3.3.6. Stage 6 of heat recovery (economizer EX-ECO)

The sixth heat transfer stage is the economizer (EX-ECO), where the main sulfur dioxide stream is further cooled from the temperature range of 465-475 °C to 260-270 °C. The cooling stream for this exchanger is supplied from two sources: a mixture of the the make-up water and a portion of the liquid outlet stream from the reboiler. This combined stream enters the exchanger at 185 °C and a pressure of 38.3 bar. After heat exchange, the cooling stream leaves at 215 °C, remaining in the liquid phase, and is then routed back to the reboiler vessel.

3.4. Pumps and blowers

Several pumps are installed in the plant to increase the static head or pressure of process streams and to ensure proper fluid transportation throughout the piping network. To provide a stable and sufficient supply of air to the Furnace, an air blower is installed on the inlet air pipeline.

For the liquid sulfur feed, a pumping system is used to transfer the sulfur and to raise its pressure to 24.5 bar before entering the furnace. In addition, another pumping system, consisting of two pumps (Pump A and Pump B), is employed to direct the main liquid stream from the separator to the first stage of heat recovery in the furnace (EX-EVAP1).

Another pumping system (including Pump A and Pump B) is responsible for supplying the main feed water to the unit. This feed water stream is mixed with a portion of the liquid outlet from reboiler before being introduced to the final stage of heat recovery in the furnace, namely the economizer (EX-ECO).

3.5. Valves and instruments

Several valves and instruments are installed throughout the unit to control and maintain the proper condition of the process. After the liquid sulfur is pressurized by Pump A and

Pump B, its pressure is reduced to 4.45 bar before entering the furnace by an electrically actuated valve (solenoid valve). Electrically actuated on/off valves are typically used for automatic control or safety isolation purposes within the process. The inlet heating coil stream in the separator is equipped with a temperature control valve, TCV, which regulates the flow to provide additional heating for the outlet heating coil stream directed to superheater EX-SUP2. In addition, the main cooling pipeline for the first heat exchanger (evaporator EX-EVAP1) is divided into two branches. The valve TCV controls the distribution of this stream, directing a portion to mix with the main water feed from reboiler 2 to supply the cooling duty required in the economizer EX-ECO.

Two pressure safety valves, PSV A and PSV B, are installed on the separator to act against overpressure conditions. A flow control valve, FCV B, is installed on the inlet air pipeline, before the air blower VN, to regulate the air flow. In addition, numerous hand valves (HV) are installed along the pipelines to allow manual control of the streams for operation or maintenance.

4. Simulation of the sulfur dioxide production unit in Aspen Plus

The Aspen Plus Software V.14 was used to simulate the sulfur oxides production plant. The main criteria to choose this software to simulate this process are its ability to provide reliable simulation for reacting systems, phase equilibria, and energy integration [39], [38]. A steady-state approach was adopted for the simulation, assuming constant operating conditions and neglecting transient effects. In addition, sensitivity analyses on key operating parameters, including air humidity, furnace temperature, and heat recovery conditions, were performed. These analyses provide useful information about operating variables and Sulfur dioxide concentration, sulfur trioxide formation, sulfuric acid formation, and acid dew point temperature.

4.1. Properties method

The thermodynamic model is of key importance for the simulation to represent the real process behavior. The ELECNRTL (Electrolyte Non-Random Two-Liquid) model was selected to accurately represent the thermodynamic behavior of systems with electrolyte formation and strong non-ideal interactions. In processes containing sulfur, especially those involving SO_2, SO_3, water and sulfuric acid, dissociation and ionic interactions are important for phase equilibrium and thermodynamic properties. The ELECNRTL model considers long-range electrostatic and short-range molecular interactions, and it is thus appropriate for the modelling of acid formation and aqueous electrolyte systems. The effect on predictions in the high-temperature gas phase is small, but it enhances the reliability of the results in regions where condensation and acid formation occur and is consistent with industrial modelling practices for the sulfuric acid process [40] [38].

The process was simulated in a steady state mode. The sulfur is burnt at approximately 1700 °C and then progressively cooled through six heat exchangers: evaporator 1 (EX-EVAP1), evaporator 2 (EX-EVAP2), superheater 2 (EX-SUP2), superheater 1 (EX-SUP1), evaporator 3 (EX-EVAP3), and economizer (EX-ECO). The gas temperature is lowered stepwise to the temperature ranges of 915-925 °C, 730-740 °C, 520-530 °C, 465-475 °C and 260-270 °C, respectively.

Chemical reactions were considered up to 734 C, from heat exchangers EX-EVAP1 to EX-SUP2. Three reactor blocks were incorporated in Aspen Plus in conjunction with the first three cooling stages.

Within the intermediate temperature range at of the third heat exchanger, the partial oxidation of SO_2 to SO_3 becomes thermodynamically feasible, and in the presence of water vapor sulfuric acid formation may occur leading to potential corrosion [1]. Downstream of this region, no significant reactions are expected. Therefore, the last three units were modelled solely as heat exchangers. The reactor sections were represented using RGibbs reactor blocks, enabling equilibrium calculations under specified thermal conditions.

The separator was modeled in Aspen Plus using a Flash2 block to represent the phase separation. In this equipment, the heat coil stream operates at a higher temperature compared to the other streams. It is responsible for supplying the required cooling liquid for heat transfer in the unit. Since the internal coil system cannot be modelled in Aspen

Plus, an equivalent representation was adopted using two external heat exchangers, namely HX-C_IN and HX-C_OUT.

The inlet coil stream is first passed through HX-C_IN to release heat and the corresponding outlet coil stream is then passed through HX-C_OUT to complete the thermal loop. These two exchangers are connected by an energy stream, where heat is transferred from the coil inlet stream to the target process stream and back to the separator. The modelling approach ensures the correct heat balance in the separator-reboiler system and the preservation of the heating role.

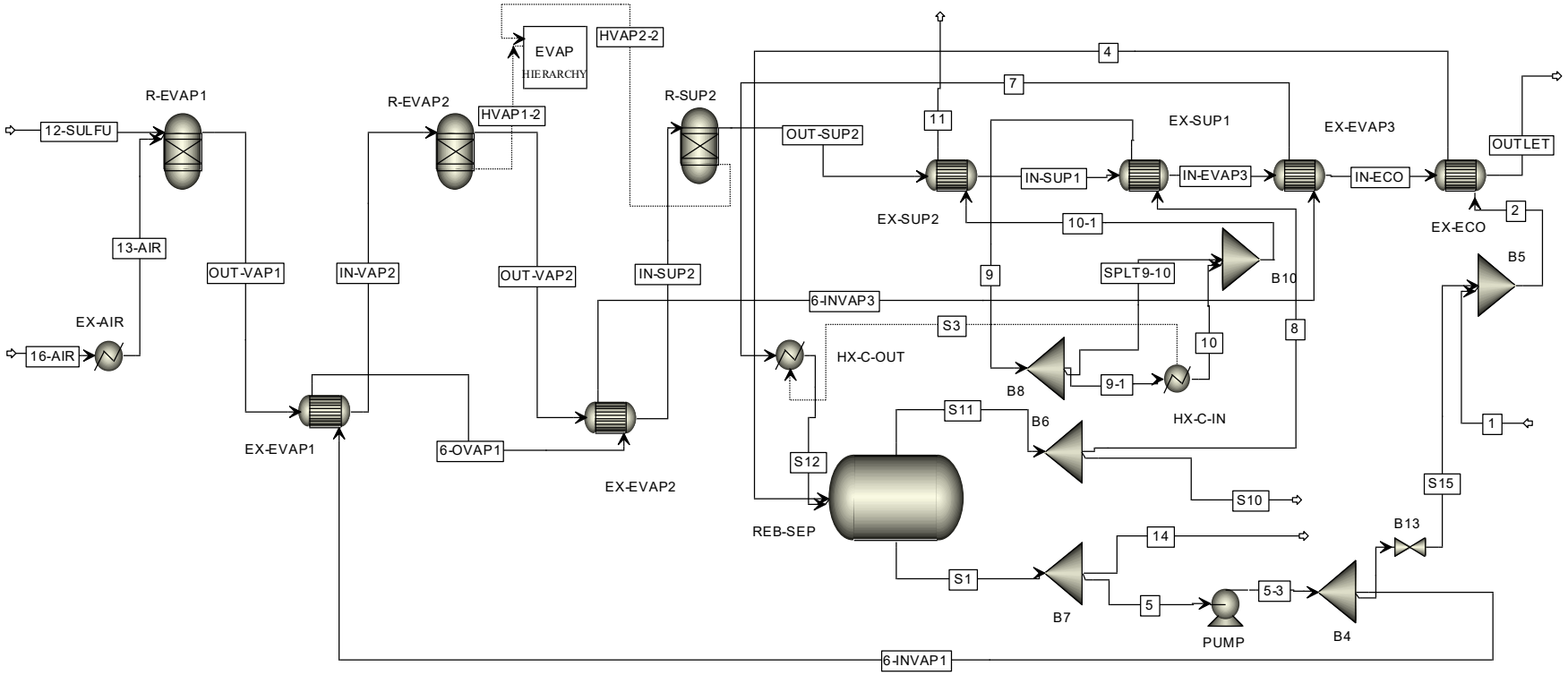

Figure 5-Sulfur dioxide production plant

4.2. Design specs

The Aspen Plus design specifications are used to modify selected flowsheet variables to specify desired process conditions. In this method, a dependent variable (e.g. temperature, flow rate or composition) is set to a desired value. On the other hand, this requirement is fulfilled by the simulator changing one or more variables. This functionality is often used when it is not possible to directly specify process variables due to interactions between unit operations and stream properties [39].

In the present model, a design specification was implemented to control the temperature of the inlet cooling stream to the economizer (EX-ECO), operating at 185 °C. This stream (Stream 2) is formed by mixing two sources: the main feed water stream (Stream 1), which originates from reboiler 2, and a portion of the liquid outlet stream from the separator–reboiler. The liquid stream from the reboiler is split into two portions. The first one is directed to the first heat exchanger (evaporator EX-EVAP1), and the second is combined with Stream 1 to form the economizer inlet cooling stream.

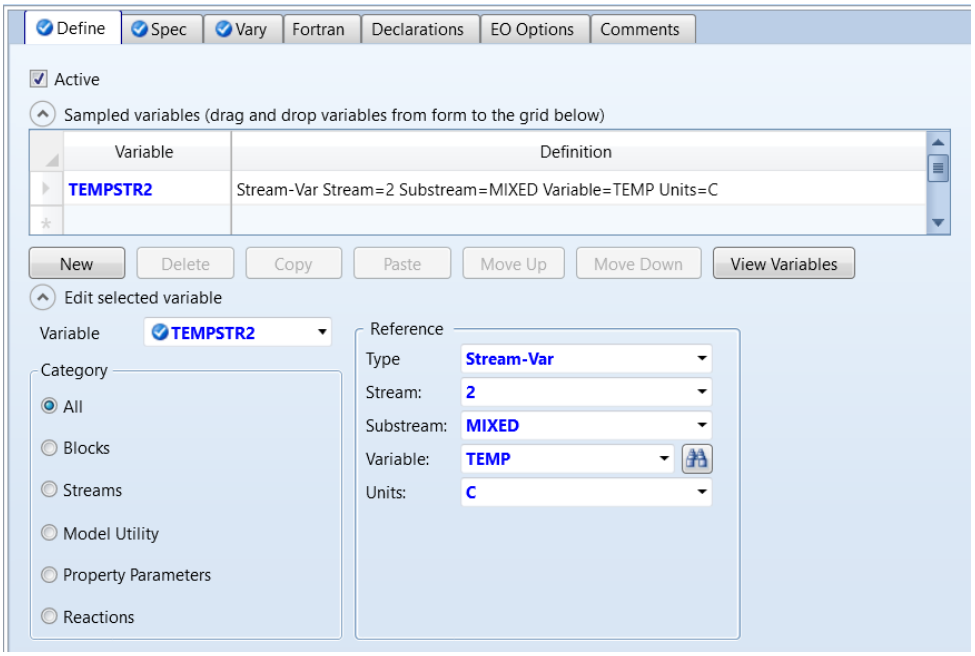

Figure 6-Design spec 1 define tab

The design spec was named as TEMPSTR2, and the target is set to 185 °C.

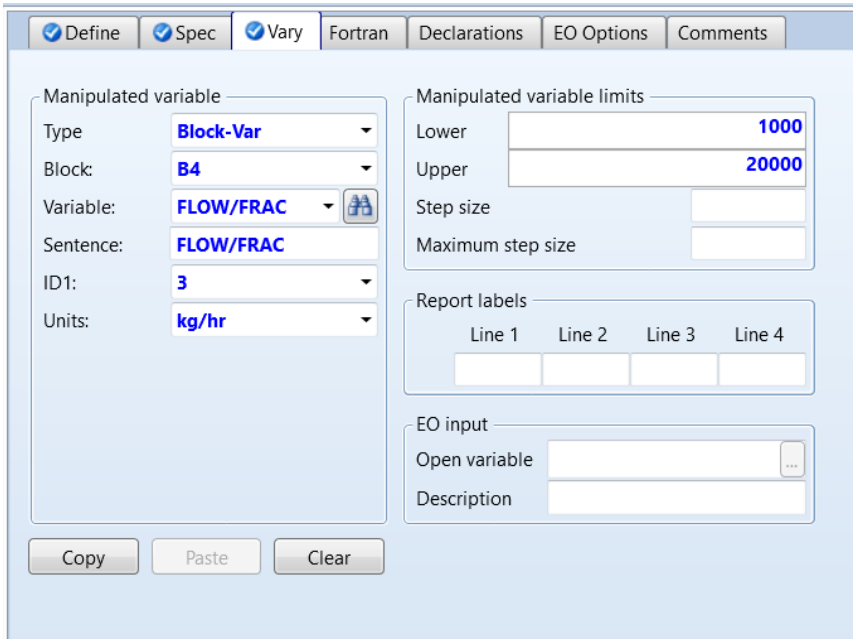

Figure 7- Design spec 1 vary tab

A second design specification was added to control the outlet temperature of superheater 2 (EX-SUP2) which needs to deliver a stream at 450 °C for downstream use in another section of the plant. In this case, Stream 9 is the superheater 1 (EX-SUP1) outlet, which is the inlet coil stream to the separator–reboiler. A portion of this stream is diverted through a valve and mixed with Stream 10, the outlet of the coil system, prior to entering superheater 2 (EX-SUP2). The mixed stream is then heated in EX-SUP2 to obtain the final outlet Stream 11.

Stream 11 temperature is considered as the controlled variable to define a design specification. The objective is to ensure that the outlet temperature of stream 11 reaches the required superheated temperature of 450 °C for power generation. Stream 9 split fraction which is controlled by valve, TCV, is considered the manipulated variable for this task by adjusting a specific portion of Stream 9 to mix with Stream 10.

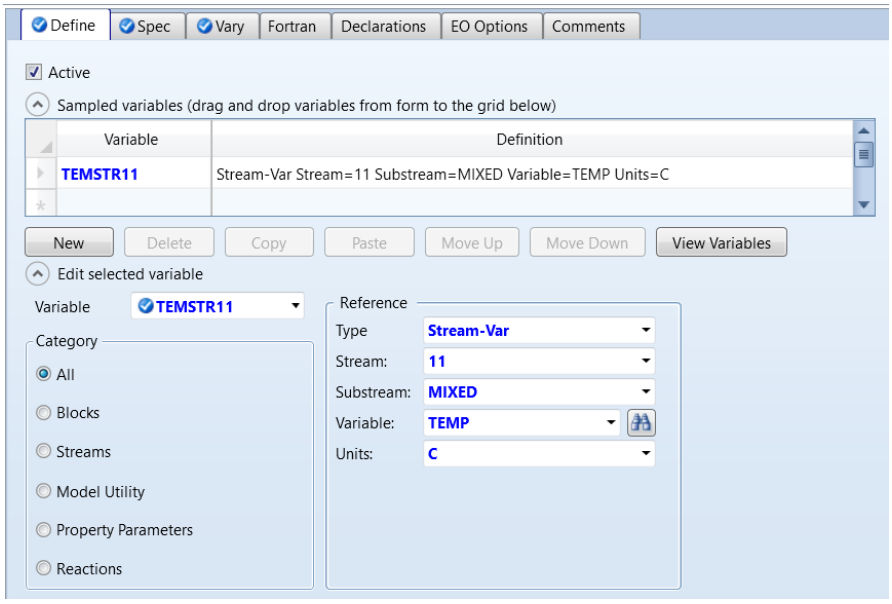

Figure 8-Design spec 2 define tab

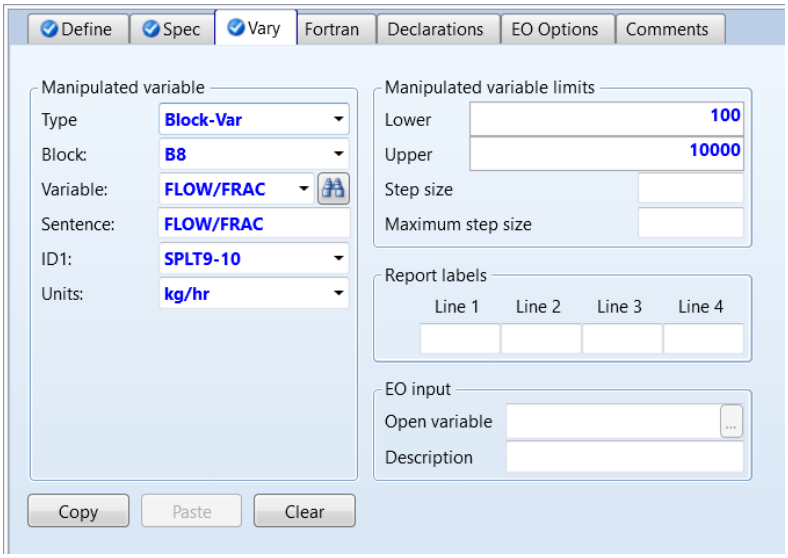

Figure 9- Design spec 2 vary tab

4.3. Sensitivity analysis

The tool proves useful for process simulation to evaluate the effect of changes in selected input parameters on the system. This method in Aspen Plus allows systematic variation

of selected variables and monitoring of changes in process outputs. It is commonly used to identify the most influential operating parameters, assess process behavior under different conditions, and support process optimization and design [39], [38].

In the present work, four sensitivity analysis scenarios were investigated in Aspen Plus to evaluate the effect of key operating parameters on the sulfur dioxide production unit. For each scenario, eleven process variables were monitored and recorded in the Define form. These variables were selected to reflect the main thermal and compositional changes occurring in the process, and the corresponding results for each variation are presented in Table 5.

In the first scenario, the effect of humidity was studied by increasing the water content of the inlet air stream. This was implemented by increasing the mass flow rate of water associated with the inlet air. The resulting changes were then evaluated through the selected process variables. Particular attention was given to the effect of humidity on the formation of sulfuric acid (H_2SO_4), since water content is directly related to corrosion risk and undesired side reactions in the system.

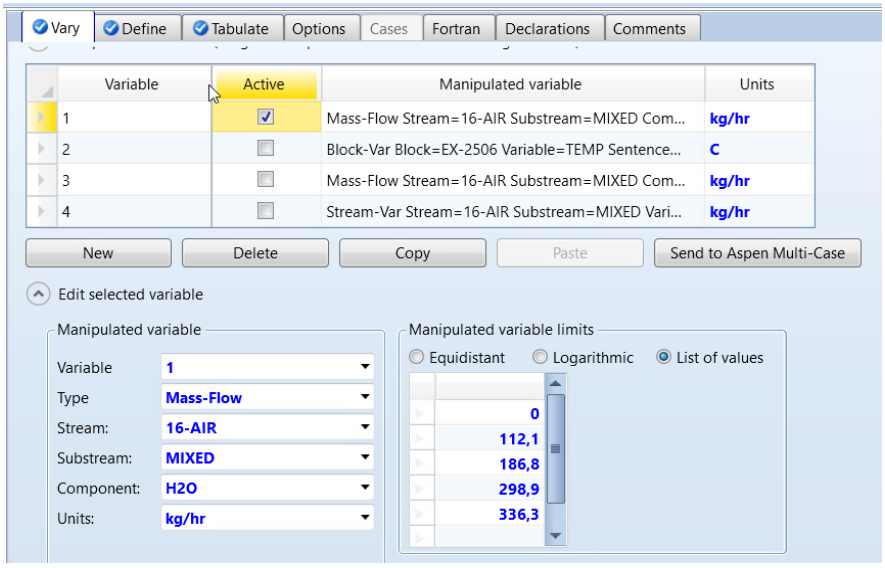

Figure 10-Sensitivity analysis case 1

Table 5 summarizes the selected process variables used in the sensitivity analysis with their definitions and specified conditions.

Table 5- Sensitivity analysis variable in the define tab

Column No.	Variable	Definition
1	YO2IN	Mole-Frac Stream=16-AIR Substream=MIXED Component=O2
2	YN2IN	Mole-Frac Stream=16-AIR Substream=MIXED Component=N2
3	YO2	Mole-Frac Stream=OUT-SUR2 Substream=MIXED Component=O2
4	YSO2	Mole-Frac Stream=OUT-SUR2 Substream=MIXED Component=SO2
5	YSO3	Mole-Frac Stream=OUT-SUR2 Substream=MIXED Component=SO3
6	YH2O	Mole-Frac Stream=OUT-SUR2 Substream=MIXED Component=H2O
7	BURNOUTT	Stream-Var Stream=OUT-VAP1 Substream=MIXED Variable=TEMP Units=C
8	VAP1FRAC	Stream-Var Stream=EVAP.6-1 Substream=MIXED Variable=VFRAC
9	VAP2FRAC	Stream-Var Stream=EVAP.6-2 Substream=MIXED Variable=VFRAC
10	VAP3FRAC	Stream-Var Stream=EVAP.7 Substream=MIXED Variable=VFRAC
11	VF6OVAP1	Stream-Var Stream=6-OVAP1 Substream=MIXED Variable=VFRAC
12	MH2SO4	Mass-Flow Stream=OUT-SUR2 Substream=MIXED Component=H2SO4 Units=kg/hr
13	MH2OOUT	Mass-Flow Stream=OUTLET Substream=MIXED Component=H2O Units=kg/hr
14	YH2SO4	Mass-Frac Stream=OUT-SUR2 Substream=MIXED Component=H2SO4

Table 6 summarizes the variables monitored during the sensitivity analysis together with the expressions used in Aspen Plus. Presenting the parameters in tabulated form made it easier to compare the effect of changing operating conditions on process behavior and outlet composition.

Table 6- Sensitivity analysis tabulated form

Column No.	Tabulated variable or expression
1	YO2IN
2	YN2IN
3	yn2in/yo2in
4	YO2*100
5	YSO2*100
6	YSO3*100
7	YH2O*100
8	BURNOUTT
9	VAP1FRAC
10	VAP2FRAC
11	VAP3FRAC
12	VF6OVAP1
13	MH2SO4
14	MH2OOUT
15	YH2SO4

The second sensitivity analysis focused on the effect of inlet-air temperature. The air temperature was increased gradually from 100 °C to 200 °C to evaluate its influence on furnace behavior, outlet gas temperature, and sulfuric acid formation and acid dew point temperature during cooling.

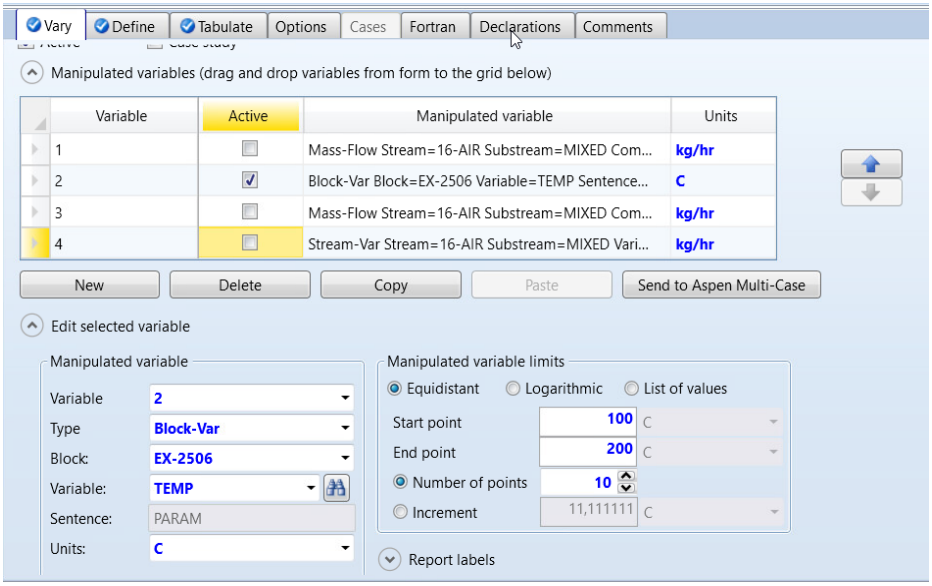

Figure 11-Sensitivity analysis case 2

The third sensitivity case examined the influence of oxygen concentration in the inlet air stream. The oxygen content was varied between 0.21 and 0.27 in order to investigate the formation tendency of SO_3 and the resulting sulfuric acid condensation risk. Increasing excess oxygen promotes additional oxidation of SO_2 to SO_3, which may increase the sulfuric acid dew point during downstream cooling.

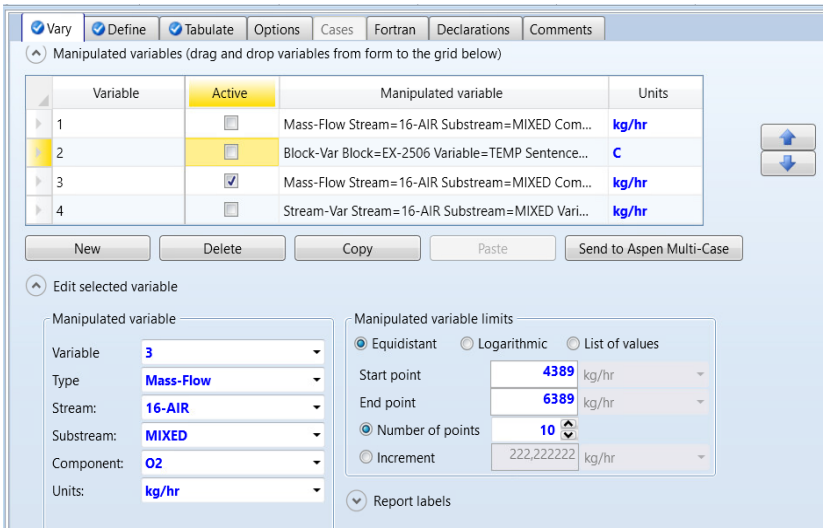

Figure 12-Sensitivity analysis case 3

The fourth sensitivity analysis investigated the effect of increasing inlet-air flow rate from 18,000 kg/h to 23,000 kg/h. The analysis focused on the resulting changes in SO_2 concentration, SO_3 formation, excess oxygen content, and sulfuric acid dew point temperature.

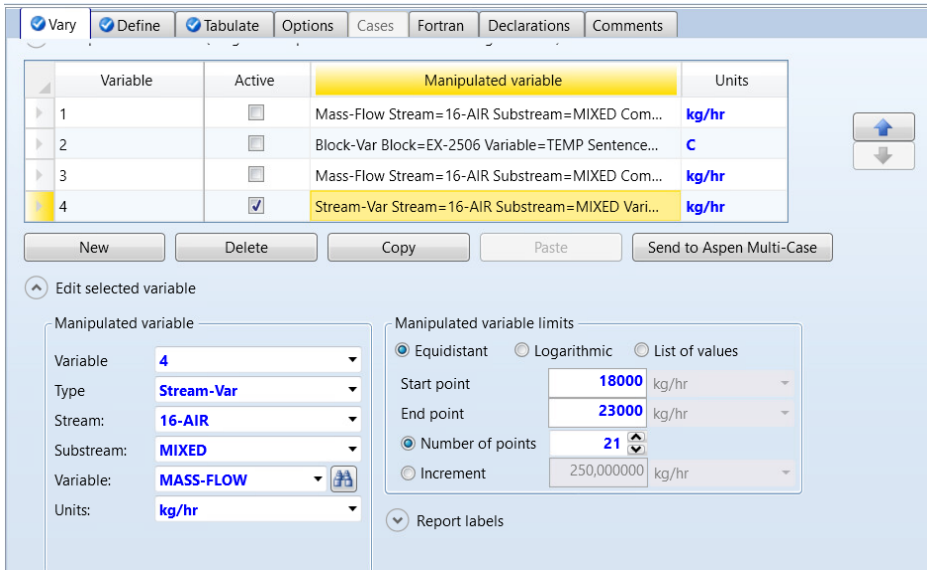

Figure 13-Sensitivity analysis case 4

5. Heat transfer surface area and overall heat transfer coefficient estimation

The heat-transfer surface area of the furnace exchangers was estimated from the external surface of the tube bundles. Although the exchangers are located inside the furnace and have an unconventional geometry, the same basic heat-transfer relation can be applied:

$$Q = UA\Delta T_{lm} \tag{5.1}$$

where Q is the heat duty, U is the overall heat-transfer coefficient, A is the heat-transfer surface area, and ΔT_{lm} is the log-mean temperature difference. The external surface area of bare tubes was calculated from:

$$A = \pi D_o L \tag{5.2}$$

where D_o is the outside tube diameter and L is the developed tube length. For U-bends, the developed bend length was estimated as:

$$L_{bend} = \pi R \tag{5.3}$$

where R is the radius of the bend. The local heat-transfer coefficient h and the overall heat-transfer coefficient U are different. The coefficient h describes heat transfer on one side of the surface, while U includes all thermal resistances, including gas side convection, tube-wall conduction, water/steam side convection, fouling and the effect of extended surfaces. For bare-tube exchangers, since the system is mainly gas-side controlled and no extended surface correction is required, the calibrated U-value can be considered approximately equivalent to the effective gas-side coefficient:

$$h \approx U \tag{5.4}$$

For studded tubes (tubes with fins), this assumption is not valid because the added fin surface is not fully effective. A temperature gradient develops along each stud, and

therefore, the effective area must be corrected by pin-fin efficiency. The pin-fin efficiency was estimated using:

$$\eta_f = \frac{\tanh(mL_c)}{mL_c} \tag{5.5}$$

$$m = \sqrt{\frac{4h}{kd_s}} \tag{5.6}$$

$$L_c = H + \frac{d_s}{4} \tag{5.7}$$

where d_s is the stud diameter, H is the stud height, $k$is the thermal conductivity of the stud material, and h is the gas-side heat-transfer coefficient. The effective heat-transfer area is then:

$$A_{eff} = A_{bare} + \eta_f(A_{doc} - A_{bare}) \tag{5.8}$$

and the overall coefficient on the documented area basis is:

$$U = h\frac{A_{eff}}{A_{doc}} \tag{5.9}$$

For studded exchangers, h was therefore obtained by reverse calculation, so that the final U-value matched the calibrated Aspen Plus value.

5.1. EX-EVAP1 — evaporator 1

For EX-EVAP1, the tube outside diameter is:

$$D_o = 168.3 \text{ mm} = 0.1683 \text{ m} \tag{5.10}$$

The exchanger contains 20 straight tubes, each 6.150 m long, therefor the total length and area can be calculated as it is shown in equation (5.11).

$$L = 20(6.150) = 123.0 \text{ m} \tag{5.11}$$

$$A = \pi(0.1683)(123.0) = 65.03\ \text{m}^2 \tag{5.12}$$

No studded-surface information was identified for this exchanger; therefore, it was treated as a bare-tube unit. Since no extended surface is present, the gas-side coefficient was considered approximately equal to the overall coefficient:

$$h \approx U \tag{5.13}$$

The calibrated Aspen Plus heat-transfer coefficients obtained for the exchanger are summarized in equations (5.14) to (5.16).

$$U_{\text{vapor-liquid}} = h_{\text{vapor-liquid}} = 0.087\ \text{kW/m}^2\text{K} = 87\ \text{W/m}^2\text{K} \tag{5.14}$$

$$U_{\text{vapor-boiling}} = h_{\text{vapor-boiling}} = 0.087\ \text{kW/m}^2\text{K} = 87\ \text{W/m}^2\text{K} \tag{5.15}$$

$$U_{\text{vapor-vapor}} = h_{\text{vapor-vapor}} = 0.020\ \text{kW/m}^2\text{K} = 20\ \text{W/m}^2\text{K} \tag{5.16}$$

5.2. EX-EVAP2 — evaporator 2

For EX-EVAP2 the tube outside diameter is:

$$D_o = 0.1683\ \text{m} \tag{5.17}$$

The total straight length is:

$$L = 22(4.206) + 2(4.975) = 102.482\ \text{m} \tag{5.18}$$

$$A = \pi(0.1683)(102.482) = 54.18\ \text{m}^2 \tag{5.19}$$

This exchanger was also treated as a bare tube because no studded-surface specification was identified. Therefore:

$$h \approx U \tag{5.20}$$

The Aspen-calibrated values for Vapor-Liquid, Vapor-Boiling, and Vapor-Vapor are listed in equations (5.21) to (5.23).

$$U_{\text{vapor-liquid}} = h_{\text{vapor-liquid}} = 0.029\ \text{kW/m}^2\text{K} = 29\ \text{W/m}^2\text{K} \quad (5.21)$$

$$U_{\text{vapor-boiling}} = h_{\text{vapor-boiling}} = 0.029\ \text{kW/m}^2\text{K} = 29\ \text{W/m}^2\text{K} \quad (5.22)$$

$$U_{\text{vapor-vapor}} = h_{\text{vapor-vapor}} = 0.020\ \text{kW/m}^2\text{K} = 20\ \text{W/m}^2\text{K} \quad (5.23)$$

5.3. EX-SUP2 — superheater 2

For EX-SUP2 the tube outside diameter is:

$$D_o = 48.3\ \text{mm} = 0.0483\ \text{m} \quad (5.24)$$

Each tube contains four straight sections of 3.841 m and three U-bends of radius 0.038 m:

$$L_{straight} = 4(3.841) = 15.364\ \text{m} \quad (5.25)$$

$$L_{bend} = 3\pi(0.038) = 0.358\ \text{m} \quad (5.26)$$

$$L_{tube} = 15.364 + 0.358 = 15.722\ \text{m} \quad (5.27)$$

$$A_1 = \pi(0.0483)(15.722) = 2.39\ \text{m}^2 \quad (5.28)$$

For 18 tubes:

$$A_{total} = 18(2.39) = 43.0\ \text{m}^2 \quad (5.29)$$

The documented area is 44.6 m², so the documented value was used in Aspen Plus:

$$A = 44.6\ \text{m}^2 \quad (5.30)$$

Since this exchanger is a bare tube:

$$h \approx U \tag{5.31}$$

The Aspen-calibrated values for Vapor-Liquid, Vapor-Boiling, and Vapor-Vapor are listed in equations (5.32) to (5.34):

$$U_{\text{vapor-liquid}} = h_{\text{vapor-liquid}} = 0.070 \text{ kW/m}^2\text{K} = 70 \text{ W/m}^2\text{K} \tag{5.32}$$
$$U_{\text{vapor-boiling}} = h_{\text{vapor-boiling}} = 0.070 \text{ kW/m}^2\text{K} = 70 \text{ W/m}^2\text{K} \tag{5.33}$$
$$U_{\text{vapor-vapor}} = h_{\text{vapor-vapor}} = 0.033 \text{ kW/m}^2\text{K} = 33 \text{ W/m}^2\text{K} \tag{5.34}$$

5.4. EX-SUP1 — superheater 1

For EX-SUP1 the tube outside diameter is:

$$D_o = 0.0483 \text{ m} \tag{5.35}$$

Each tube contains eight straight sections of 3.841 m and seven U-bends of radius 0.038 m:

$$L_{straight} = 8(3.841) = 30.728 \text{ m} \tag{5.36}$$
$$L_{bend} = 7\pi(0.038) = 0.836 \text{ m} \tag{5.37}$$
$$L_{tube} = 30.728 + 0.836 = 31.564 \text{ m} \tag{5.38}$$
$$A_1 = \pi(0.0483)(31.564) = 4.79 \text{ m}^2 \tag{5.39}$$

For 18 tubes:

$$A_{total} = 18(4.79) = 86.2 \text{ m}^2 \tag{5.40}$$

The documented area is 87.0 m², which confirms the bare-tube basis:

$$A = 87.0 \text{ m}^2 \tag{5.41}$$

The calibrated Aspen Plus heat-transfer coefficients obtained for the exchanger are summarized in equations (5.42) to (5.44).

$$U_{\text{vapor-liquid}} = h_{\text{vapor-liquid}} = 0.068\ \text{kW/m}^2\text{K} = 68\ \text{W/m}^2\text{K} \quad (5.42)$$

$$U_{\text{vapor-boiling}} = h_{\text{vapor-boiling}} = 0.068\ \text{kW/m}^2\text{K} = 68\ \text{W/m}^2\text{K} \quad (5.43)$$

$$U_{\text{vapor-vapor}} = h_{\text{vapor-vapor}} = 0.068\ \text{kW/m}^2\text{K} = 68\ \text{W/m}^2\text{K} \quad (5.44)$$

5.5. EX-EVAP3 — evaporator 3, studded tube

For EX-EVAP3, the bare-tube area was first calculated. The tube outside diameter is:

$$D_o = 168.3\ \text{mm} = 0.1683\ \text{m} \quad (5.45)$$

The exchanger contains 10 straight pipes of 3.578 m and two inlet/outlet pipes of 4.975 m:

$$L_{straight} = 10(3.578) + 2(4.975) = 45.73\ \text{m} \quad (5.46)$$

The bend contribution was estimated using:

$$R = \frac{219}{2} = 0.1095\ \text{m} \quad (5.47)$$

$$L_{bend} = 11\pi(0.1095) = 3.784\ \text{m} \quad (5.48)$$

$$L_{total} = 45.73 + 3.784 = 49.514\ \text{m} \quad (5.49)$$

$$A_{bare} = \pi(0.1683)(49.514) = 26.18\ \text{m}^2 \quad (5.50)$$

The documentation states:

Number of studs = 4920 studs per tube (5.51)

Number of Stud per meter = 1375 stud/m (5.52)

The studded length is:

$$L = \frac{4920}{1375} = 3.578 \text{ m} \tag{5.53}$$

which matches the 3578 mm pipe length. Therefore, the 10 straight pipes were considered studded.

The stud circle outside diameter is 219 mm, so the stud height is:

$$H = \frac{219 - 168.3}{2} = 25.35 \text{ mm} = 0.02535 \text{ m} \tag{5.54}$$

Assuming a stud diameter of:

$$d_s = 12.7 \text{ mm} = 0.0127 \text{ m} \tag{5.55}$$

The area of one cylindrical stud was estimated as:

$$A_{stud} = \pi d_s H + \frac{\pi d_s^2}{4} \tag{5.56}$$

$$A_{stud} = \pi(0.0127)(0.02535) + \frac{\pi(0.0127)^2}{4} \tag{5.57}$$

$$A_{stud} = 0.001138 \text{ m}^2 \tag{5.58}$$

The total number of studs is:

$$N_{stud} = 10(4920) = 49200 \tag{5.59}$$

$$A_{stud,total} = 49200(0.001138) = 55.99 \text{ m}^2 \tag{5.60}$$

Thus, the directly calculated geometric studded area is:

$$A_{geom} = 26.18 + 55.99 = 82.17 \text{ m}^2 \tag{5.61}$$

However, the combined documented area for EX-EVAP1, EX-EVAP2, and EX-EVAP3 is 207.9 m². Since EX-EVAP1 and EX-EVAP2 were treated as bare-tube exchangers:

$$A_{EX-2502C} = 207.9 - 65.03 - 54.18 \tag{5.62}$$

$$A_{EX-2502C} = 88.69 \text{ m}^2 \tag{5.63}$$

The difference between the direct stud calculation and the document-based value is:

$$A_{difference} = 88.69 - 82.17 = 6.52 \text{ m}^2 \tag{5.64}$$

This difference was assigned to EX-EVAP3 to remain consistent with the equipment documentation. The thermal conductivity of ASTM A335 P22 was assumed as:

$$k = 35 \text{ W/mK} \tag{5.65}$$

Solving the pin-fin relation gives:

$$h = 20.69 \text{ W/m}^2\text{K} \tag{5.66}$$

$$L_c = 0.02535 + \frac{0.0127}{4} = 0.02853 \text{ m} \tag{5.67}$$

$$m = \sqrt{\frac{4(20.69)}{35(0.0127)}} = 13.66 \text{ m}^{-1} \tag{5.68}$$

$$mL_c = 13.66(0.02853) = 0.390 \tag{5.69}$$

$$\eta_f = \frac{\tanh(0.390)}{0.390} = 0.952 \tag{5.70}$$

$$A_{eff} = 26.18 + 0.952(88.69 - 26.18) = 85.71 \text{ m}^2 \tag{5.71}$$

$$U = 20.69\frac{85.71}{88.69} = 20.0 \text{ W/m}^2\text{K} \tag{5.72}$$

$$U = 0.020 \text{ kW/m}^2\text{K} \tag{5.73}$$

5.6. EX-ECO — economizer, studded tube

For the economizer, the bare-tube area was calculated previously as:

$$A_{bare} = 122.3 \text{ m}^2 \tag{5.74}$$

The documented area is:

$$A_{doc} = 359.0 \text{ m}^2 \tag{5.75}$$

The documentation confirms studded tubes:

Number of studs = 2742 studs per tube (5.76)
Number of Stud per meter = 750 stud/m (5.77)

The studded length is:

$$L = \frac{2742}{750} = 3.656 \text{ m} \tag{5.78}$$

The pipe outside diameter is 114.4 mm, and the outside diameter of the stud circle is 165 mm. Therefore, the stud height is:

$$H = \frac{165 - 114.4}{2} = 25.3 \text{ mm} = 0.0253 \text{ m} \tag{5.79}$$

assuming:

$$d_s = 12.7 \text{ mm} = 0.0127 \text{ m} \tag{5.80}$$

The area of one stud is:

$$A_{stud} = \pi d_s H + \frac{\pi d_s^2}{4} \tag{5.81}$$

$$A_{stud} = 0.001136 \text{ m}^2 \tag{5.82}$$

The studded geometry confirms that the documented area is significantly larger than the bare-tube area. Therefore:

$$A = 359.0 \text{ m}^2 \tag{5.83}$$

The Aspen-calibrated coefficient is:

$$U = 0.025 \text{ kW/m}^2\text{K} = 25 \text{ W/m}^2\text{K} \tag{5.84}$$

Carbon steel thermal conductivity was assumed to be:

$$k = 45 \text{ W/mK} \tag{5.85}$$

Solving the pin-fin relation gives:

$$h = 25.78 \text{ W/m}^2\text{K} \tag{5.86}$$

$$m = \sqrt{\frac{4(25.78)}{45(0.0127)}} = 13.43 \text{ m}^{-1} \tag{5.87}$$

$$mL_c = 13.43(0.02848) = 0.383 \tag{5.88}$$

$$\eta_f = \frac{\tanh(0.383)}{0.383} = 0.954 \tag{5.89}$$

$$A_{eff} = 122.3 + 0.954(359.0 - 122.3) = 348.09 \text{ m}^2 \tag{5.90}$$

$$U = 25.78\frac{348.09}{359.0} = 25.0 \text{ W/m}^2\text{K} \tag{5.91}$$

$$U = 0.025 \text{ kW/m}^2\text{K} \tag{5.92}$$

For bare-tube exchangers, the absence of extended surfaces allows the effective gas-side coefficient to be approximated by the Aspen-calibrated overall heat-transfer coefficient. This is reasonable because the heat-transfer resistance is dominated by the gas side. For studded exchangers, however, the added surface is not fully effective due to conduction resistance along the studs. Therefore, the fin efficiency was calculated and the gas-side coefficient was obtained. The resulting values of $h$and U are within the typical range for gas-side-controlled furnace heat-transfer equipment and provide a physically consistent basis for Aspen Plus simulation.

Table 7- Surface area and overall heat transfer coefficient

Order	Equipment	Surface type	Area used in Aspen (m2)	U vapor-liquid (kW/m2.K)	U vapor-boiling (kW/m2.K)	U vapor-vapor (kW/m2.K)	Remark
1	EX-EVAP1	Bare Tube	65.03	0.087	0.087	0.020	High-temperature evaporator

2	EX-EVAP2	Bare Tube	54.18	0.029	0.029	0.020	Medium temperature evaporator
3	EX-SUP2	Bare Tube	44.6	0.070	0.070	0.033	Superheater
4	EX-SUP1	Bare Tube	87	0.068	0.068	0.068	Superheater
5	EX-EVAP3	Fin Tube	82.03	0.020	0.020	0.020	Low-temperature evaporator
6	EX-ECO	Fin tube	346.42	0.025	0.025	0.025	Economizer

6. Heat and material balance

6.1 Material balance for sulfur dioxide production

The sulfur furnace is the main reaction unit of the process and can be treated as a steady-state reacting system. In its general form, the material balance for a reactive system is expressed as:

$$\text{Accumulation} = \text{Input} - \text{Output} + \text{Generation} - \text{Consumption} \tag{6.1}$$

or, for any species i:

$$\frac{dN_i}{dt} = \sum \dot{n}_{i,in} - \sum \dot{n}_{i,out} + \dot{n}_{i,gen} - \dot{n}_{i,cons} \tag{6.2}$$

Under steady-state conditions, the accumulation term is zero, and the balance reduces accordingly. On an overall mass basis, this simplifies to $\sum \dot{m}_{in} = \sum \dot{m}_{out}$, which is commonly used to verify process consistency in industrial systems [41].

In the present case, liquid sulfur is fed to the furnace and reacts with oxygen from the air. The main reaction is the formation of sulfur dioxide. A part of the sulfur dioxide is

further oxidized to sulfur trioxide. The sulfur trioxide is then assumed to react completely with water vapor to form sulfuric acid [1], [7]:

$$S + O_2 \rightarrow SO_2 \quad (6.3)$$

$$SO_2 + \frac{1}{2}O_2 \rightarrow SO_3 \quad (6.4)$$

$$SO_3 + H_2O \rightarrow H_2SO_4 \quad (6.5)$$

The sulfur feed rate is 4140 kg/h, and the air feed rate is 19150 kg/h. The average molecular weight of air is taken as 28.75 kg/kmol. The air composition is given as:

$$O_2 = 0.206046 \quad (6.6)$$

$$N_2 = 0.765315 \quad (6.7)$$

$$Ar = 0.009812 \quad (6.8)$$

$$H_2O = 0.015526 \quad (6.9)$$

Yield represents the fraction of sulfur converted to the desired product (SO_2).

$$\text{Yield} = \frac{SO_2 \text{ formed}}{\text{theoretical } SO_2} \quad (6.10)$$

The yield for this unit is assumed to be 93.8%, and it can be calculated as it is indicated in equations (6.11) to (6.14)

Sulfur feed = 4140 kg/h (6.11)

SO_2 = 121.3912 kmol/h (6.12)

Total S = 129.375 kmol/h (6.13)

$$\text{Yield} = \frac{121.3912}{129.375} = 93.8\% \quad (6.14)$$

The production rate of sulfur dioxide is specified as 121.3912 kmol/h, and the remaining sulfur is assumed to be converted to sulfur trioxide and then fully to sulfuric acid in steady-state conditions. The equations (6.15) to (6.19) represents the basic data of the process.

Sulfur feed = 4140 kg/h (6.15)

Air feed = 19150 kg/h (6.16)

Molecular weight of sulfur = 32 kg/kmol (6.17)

Molecular weight of air = 28.75 kg/kmol (6.18)

SO_2 produced = 121.3912 kmol/h (6.19)

Material Balance for Inlet Streams is calculated in equations (6.20) to (6.26). The sulfur feed on molar basis is:

$$\dot{n}_S = \frac{4140}{32} = 129.375 \text{ kmol/h} \tag{6.20}$$

The molar flow rate of the air stream is:

$$\dot{n}_{air} = \frac{19150}{28.75} = 666.087 \text{ kmol/h} \tag{6.21}$$

Using the given air composition, the inlet oxygen flow is approximately:

$$\dot{n}_{O_2,in} = 137.699 \text{ kmol/h} \tag{6.22}$$

which corresponds to:

$$\dot{m}_{O_2,in} = 137.699 \times 32 = 4406.37 \text{ kg/h} \tag{6.23}$$

To preserve the total air feed of 19150 kg/h, the remaining air mass is distributed among nitrogen, argon, and water vapor as it is written in equations (6.24) to (6.26).

$$N_2 = 14295.54 \text{ kg/h} \tag{6.24}$$

$$Ar = 261.49 \text{ kg/h} \tag{6.25}$$

$$H_2O = 186.60 \text{ kg/h} \tag{6.26}$$

The inlet streams' flow rates for each component are provided in Table 8.

Table 8- Inlet flow rate of components (kg/h)

Component	Inlet Flow rate (kg/h)
Sulfur	4140

Oxygen	4406.37
Nitrogen	14295.54
Argon	261.49
Water Vapor	186.60
Total	23290

Material balance for the outlet stream is calculated in equations (6.27) to (6.41). The outlet sulfur dioxide flow rate is given as:

$$\dot{n}_{SO_2,out} = 121.3912 \text{ kmol/h} \quad (6.27)$$

which corresponds to:

$$\dot{m}_{SO_2,out} = 121.3912 \times 64 = 7769.04 \text{ kg/h} \quad (6.28)$$

The remaining sulfur is first converted to sulfur trioxide:

$$\dot{n}_{SO_3} = 129.375 - 121.3912 = 7.9838 \text{ kmol/h} \quad (6.29)$$

Since Sulfur trioxide is assumed to react completely with water vapor, the sulfuric acid formed is:

$$\dot{n}_{H_2SO_4,out} = 7.9838 \text{ kmol/h} \quad (6.30)$$

$$\dot{m}_{H_2SO_4,out} = 7.9838 \times 98 = 782.41 \text{ kg/h} \quad (6.31)$$

The water consumed in this reaction is equal to the SO_3 converted:

$$\dot{n}_{H_2O,cons} = 7.9838 \text{ kmol/h} \quad (6.32)$$

$$\dot{m}_{H_2O,cons} = 7.9838 \times 18 = 143.71 \text{ kg/h} \quad (6.33)$$

Therefore, the remaining water vapor in the outlet stream is:

$$\dot{m}_{H_2O,out} = 186.60 - 143.71 = 42.89 \text{ kg/h} \quad (6.34)$$

For oxygen, the total consumption includes sulfur oxidation to SO_2 and the further oxidation of part of SO_2 to SO_3:

$$\dot{n}_{O_2,cons} = 129.375 + 0.5(7.9838) = 133.3669 \text{ kmol/h} \quad (6.35)$$

The unreacted oxygen leaving the system is:

$$\dot{n}_{O_2,out} = 137.699 - 133.3669 = 4.3321 \text{ kmol/h} \quad (6.36)$$

$$\dot{m}_{O_2,out} = 4.3321 \times 32 = 138.63 \text{ kg/h} \quad (6.37)$$

Nitrogen and argon are assumed to be inert:

$$N_2 = 14295.54 \text{ kg/h} \quad (6.38)$$

$$Ar = 261.49 \text{ kg/h} \quad (6.39)$$

The outlet streams' flow rates for each component are provided in Table 9.

Table 9- Outlet flow rate of components (kg/h)

Component	Outlet flow rate (kg/h)
Sulfur Dioxide	7769.04
Sulfuric acid	782.41
Oxygen	138.63
Nitrogen	14295.54
Argon	261.49
Water Vapor	42.89
Total	23290

The overall balance for Sulfur dioxide production indicates a balance in inlet and outlet mass into the system.

$$\sum \dot{m}_{in} = 23290.00 \text{ kg/h} \quad (6.40)$$

$$\sum \dot{m}_{out} = 23290.00 \text{ kg/h} \quad (6.41)$$

6.2 Energy balance for sulfur dioxide production

The energy balance is based on the first law of thermodynamics. For a steady-state open system, the general expression is [41], [38]:

$$\text{Accumulation of energy} = \dot{Q} - \dot{W} + \sum \dot{m}_{in} \widehat{H}_{in} - \sum \dot{m}_{out} \widehat{H}_{out} \quad (6.42)$$

Under steady-state conditions, the accumulation term is zero. Since no shaft work is associated with the furnace itself, the balance reduces to:

$$\dot{Q} + \sum \dot{m}_{in} \widehat{H}_{in} - \sum \dot{m}_{out} \widehat{H}_{out} = 0 \quad (6.43)$$

In this system, the total heat released is associated with three exothermic reactions [1], [7]:

$$\mathrm{S} + \mathrm{O_2} \rightarrow \mathrm{SO_2} \qquad \Delta H^\circ = -296.8 \text{ kJ/mol} \quad (6.44)$$

$$\mathrm{SO_2} + \frac{1}{2}\mathrm{O_2} \rightarrow \mathrm{SO_3} \qquad \Delta H^\circ \approx -98.9 \text{ kJ/mol} \quad (6.45)$$

$$\mathrm{SO_3} + \mathrm{H_2O} \rightarrow \mathrm{H_2SO_4} \quad \Delta H^\circ \approx -130 \text{ kJ/mol} \quad (6.46)$$

The first reaction applies to the total sulfur feed:

$$\dot{Q}_1 = 129.375 \times 296.8 \times 10^3 \text{ kJ/h} \quad (6.47)$$

$$\dot{Q}_1 = 3.840 \times 10^7 \text{ kJ/h} \quad (6.48)$$

The second reaction applies to the fraction of SO_2 converted to SO_3:

$$\dot{Q}_2 = 7.9838 \times 98.9 \times 10^3 \text{ kJ/h} \quad (6.49)$$

$$\dot{Q}_2 = 7.896 \times 10^5 \text{ kJ/h} \quad (6.50)$$

The third reaction applies to the complete conversion of SO_3 to sulfuric acid:

$$\dot{Q}_3 = 7.9838 \times 130 \times 10^3 \text{ kJ/h} \quad (6.51)$$
$$\dot{Q}_3 = 1.038 \times 10^6 \text{ kJ/h} \quad (6.52)$$

The total theoretical heat released is therefore:

$$\dot{Q}_{total} = \dot{Q}_1 + \dot{Q}_2 + \dot{Q}_3 \quad (6.53)$$
$$\dot{Q}_{total} = 3.840 \times 10^7 + 7.896 \times 10^5 + 1.038 \times 10^6 \text{ kJ/h} \quad (6.54)$$
$$\dot{Q}_{total} = 4.023 \times 10^7 \text{ kJ/h} \quad (6.55)$$

Converting this to power:

$$\dot{Q}_{total} = \frac{4.023 \times 10^7}{3600} \approx 1.118 \times 10^4 \text{ kW} \quad (6.56)$$
$$\dot{Q}_{total} \approx 11.18 \text{ MW} \quad (6.57)$$

This value represents the theoretical heat generated by sulfur combustion, partial oxidation to SO_3, and the subsequent formation of sulfuric acid.

7. Energy analysis and heat recovery

7.1 Energy analysis and pinch technology

Pinch technology is a thermodynamic method used to determine the maximum possible heat recovery inside a process before external heating or cooling utilities are required. The method combines all hot streams into a hot composite curve and all cold streams into a cold composite curve. The minimum temperature difference between these curves corresponds to the selected minimum temperature approach, ΔT_{min}, and defines the

pinch region. The Grand Composite Curve (GCC) is then generated from the heat difference between the shifted composite curves and is used to identify utility targets and possible heat recovery opportunities [42].

In this work, pinch analysis was performed using Aspen Energy Analyzer based on the heat recovery network obtained from Aspen Plus simulation. The analysis was carried out to evaluate the existing waste heat recovery performance and investigate the possibility of recovering additional low-temperature heat while maintaining the process gas temperature above the sulfuric acid dew point.

The heat transfer calculations are based on:

$$Q = MC_p\Delta T \tag{7.1}$$

where:

- Q= heat duty
- MC_p= heat-capacity flowrate
- ΔT= temperature difference

For evaporator sections, the water/steam streams absorb latent heat at nearly constant temperature and in a two-phase region. Therefore, these streams appear as nearly horizontal sections on the composite curve because a large amount of heat is transferred over a very small temperature interval.

7.2 Thermal oil loop for low-temperature heat recovery

A closed thermal oil loop was proposed to recover the remaining low-grade heat from the final SO_2-rich gas stream while maintaining the gas temperature above the sulfuric acid dew point.

For the base operating case corresponding to 4141 kg/h sulfur, the final gas temperature after the economizer is approximately $265^{\circ}C$. Based on the sensitivity analysis, the sulfuric acid dew point for this case varies approximately between 180 C to 205 C.

Therefore, the recoverable heat was conservatively limited to 265 C to 205 C. Giving an estimated recoverable heat load of approximately:

$$Q = 370\ \mathrm{kW} \tag{7.2}$$

The oil-loop heat balance is:

$$Q = \dot{m}_{oil} C_{p,oil} \Delta T_{oil} \tag{7.3}$$
$$Q = 370\ \mathrm{kW} \tag{7.4}$$
$$C_{p,oil} = 2.4\ \mathrm{kJ/kg \cdot K} \tag{7.5}$$
$$\Delta T_{oil} = 50°C \tag{7.6}$$

The required oil circulation rate are calculated in equation (7.7) to (7.8).

$$\dot{m}_{oil} = \frac{370}{2.4 \times 50}\ \mathrm{kg/s} \tag{7.7}$$
$$\dot{m}_{oil} = 3.1\ \mathrm{kg/s} \tag{7.8}$$

A practical oil operating range for the base case is 180 C to 230 °C, with an operating pressure of approximately 3 to 5 bar. The oil loop should include:

- gas–oil heat exchanger,
- oil–air or oil–water exchanger,
- circulation pump,
- expansion tank,
- bypass control valve,
- pressure relief valve.

7.3 Heat recovery with the furnace outlet stream

A key concept in process engineering is to utilize the excessive heat of the system to reduce extra energy consumption. In this process, thermal energy from high-temperature outlet streams is used to preheat colder inlet streams which reduces overall energy consumption and improves process efficiency. This approach is an important part of process integration, where internal energy sources are used before external utilities are resorted to. The recovery and utilization of waste heat not only enhances the thermal efficiency but also reduces the operational cost and environmental impact through the reduction of fuel consumption and associated emissions [38], [40].

In this section, heat recovery was implemented on the plant by utilizing the outlet stream of the furnace, which leaves the system at approximately 266 °C, as a heat source for preheating the inlet air stream. Calculating the sulfuric acid dew point temperature is an essential factor that limits the heat transfer for this heat recovery. Due to the sensitivity analysis calculation, a lower limit of 205 °C was considered for this heat recovery. In the initial configuration of the process, air preheating was carried out using a dedicated heat exchanger, where the inlet air temperature was raised to 100 °C with a heat duty of 419.155 kW. This new configuration adds a shell-and-tube heat exchanger. In this new modification, the outlet temperature of the preheated air reached 171.8 °C, increasing the air preheating temperature by more than 70 °C.

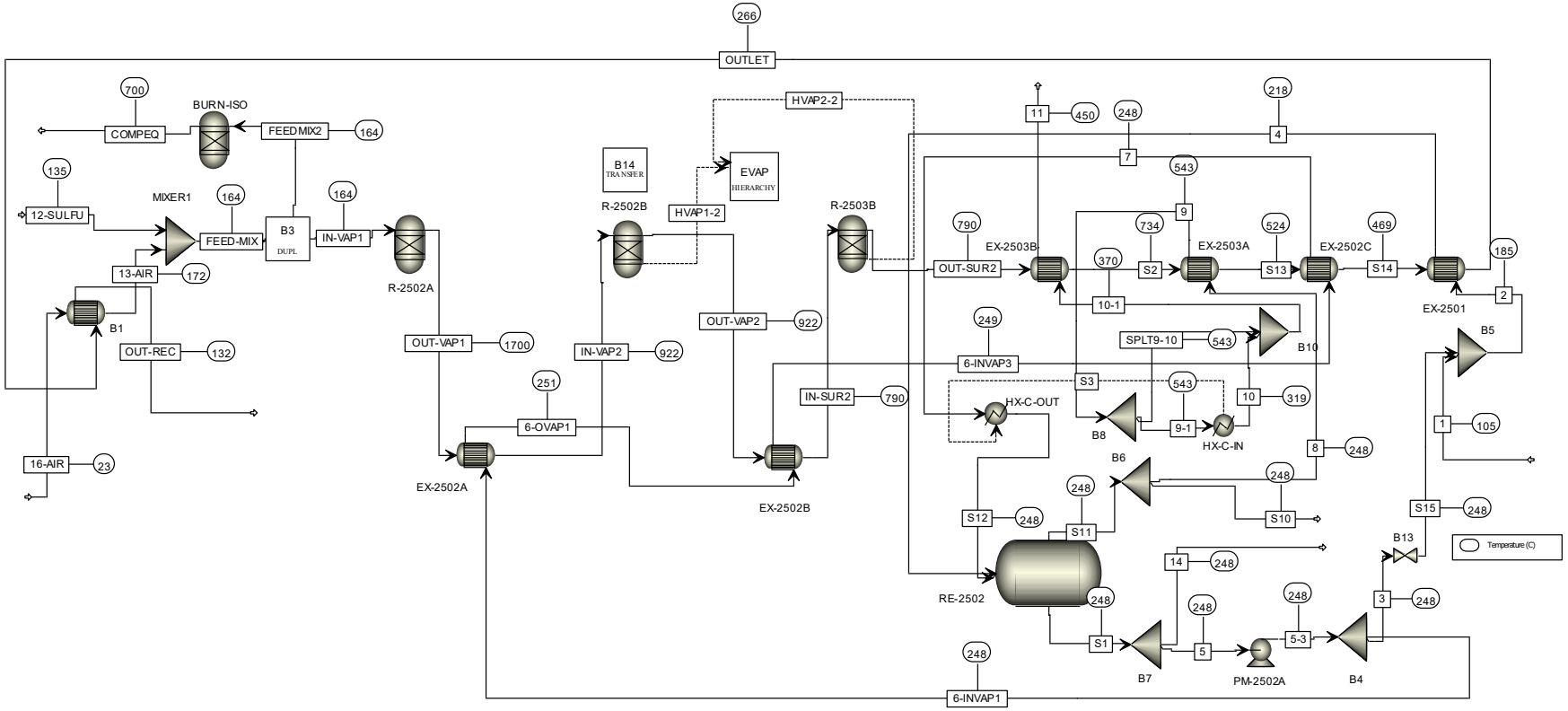

Figure 14- Heat recovery with furnace outlet

8. Results

In this section, the main simulation results from the Aspen Plus model are presented and discussed. Particular attention is given to the combustion behavior, heat recovery performance, sulfur oxide formation, and thermal behavior of the process streams in the whole plant.

8.1 Simulation results

The simulation results showed that the sulfur combustion process produces a hot sulfur dioxide-rich gas stream with a concentration of 18.23 mol%. The temperature of the process gas in the first section of the furnace is approximately 1702.9°C. The heat recovery system contains six heat exchangers to provide cooling service for the furnace. The combustion of sulfur in excess air is a highly exothermic process. The gas stream exiting the furnace contains mostly nitrogen, sulfur dioxide, sulfur trioxide, water, residual oxygen, and traces of sulfuric acid formation.

SO_3 generation is more significant at lower temperatures during downstream cooling stages. In addition, the heat duties of all three reactors were fixed at zero to allow Aspen Plus to calculate the outlet temperature directly from the heat released by the reactions.

Combustion gas temperature decreases as it passes through the heat recovery section. The gas temperature decreases from approximately 1702.9°C in evaporator 1 to approximately 265.2 °C at the economizer final outlet. This behavior confirms that a large part of the thermal energy released during combustion is recovered before the gases leave the system. On the utility side, water enters the heat recovery section in the liquid phase at approximately 185 °C and 38.32 bar.

At the Outlet stream, the outlet oxygen concentration is approximately 0.89 mol%, indicating the presence of excess oxygen after combustion. The composition profiles also reveal the presence of sulfur trioxide in the gas phase with concentrations of 1.2 mol%.

Simulation results show that the proposed process configuration has the potential to recover a significant part of the thermal energy released in the sulfur combustion, while

ensuring stable sulfur dioxide production and acceptable thermal performance of the entire heat recovery system. The industrial data were obtained from the analysis of several real industrial plants in a confidential way. Table 10 compares the industrial data with the Aspen Plus simulation results, which indicates an acceptable convergence between these two sets of data.

Table 10-Industrial data and simulation results comparison

	Industrial values	Aspen Plus simulation values
R-EVAP1 Temp C	---	1702.9
EX-EVAP1 Temp C	922	921.6
R-EVAP2 Temp C	---	934.1
EX-EVAP2 Temp C	790	797.3
R-SUP2 Temp C	---	815.1
EX-SUP2 Temp C	734	734.8
EX-SUP1 Temp C	524	524
EX-EVAP3 Temp C	469	463.2
EX-ECO Temp C	266	265.2
Excess Oxygen outlet %	0.58	0.89
Superheated steam to Turbine Temp C	450	450

Table 11-Aspen Plus simulation result

	Units	12-SULFU	16-AIR	OUT-VAP1	IN-VAP2	OUT-VAP2	IN-SUP2	OUT-SUP2	IN-SUP1	IN-EVAP3	IN-ECO	OUTLET
Description												
From				R-EVAP1	EX-EVAP1	R-EVAP2	EX-EVAP2	R-SUP2	EX-SUP2	EX-SUP1	EX-EVAP3	EX-ECO
To		R-EVAP1	EX-AIR	EX-EVAP1	R-EVAP2	EX-EVAP2	R-SUP2	EX-SUP2	EX-SUP1	EX-EVAP3	EX-ECO	
Stream Class		CONVEN	CONVEN	CONVEN	CONVEN	CONVEN	CONVEN	CONVEN	CONVEN	CONVEN	CONVEN	CONVEN
Phase		Liquid Phase	Vapor Phase	Vapor Phase	Vapor Phase	Vapor Phase	Vapor Phase	Vapor Phase	Vapor Phase	Vapor Phase	Vapor Phase	Vapor Phase
Temperature	C	135	22.5	1702.9559	921.63833	934.12333	797.328656	815.13077	734.80195	524.05082	463.27828	265.21682
Pressure	bar	24.5	1.035	1.035	1.035	1.035	1.035	1.035	1.035	1.035	1.035	1.035
Molar Vapor Fraction		0	1	1	1	1	1	1	1	1	1	1
Molar Liquid Fraction		1	0	0	0	0	0	0	0	0	0	0
Molar Enthalpy	kJ/mol	13.32236	-4.6795285	0.3209922	-30.559921	-30.63549	-35.83695	-35.96109	-38.9879	-46.72370	-48.8904	-55.7233
Mass Enthalpy	kJ/kg	415.46689	-163.31917	9.210420	-876.87394	-876.8739	-1025.7544	-1025.7545	-1112.0926	-1332.7472	-1394.5522	-1589.4533
Molar Entropy	kJ/kmol-K	-670.0638	3.7088059	73.867960	54.028301	54.203309	49.631475	49.83571	46.94662	38.34364	35.51675	24.72413
Mass Entropy	kJ/kg-K	-20.89639	0.1294401	2.1195371	1.5502660	1.5514510	1.4205922	1.421514	1.339105	1.093714	1.013080	0.705231
Molar Density	kmol/cum	62.80242	0.0421315	0.0062984	0.010416	0.0103090	0.0116263	0.011436	0.012347	0.015612	0.016900	0.023123
Mass Density	kg/cum	2013.8226	1.2071813	0.2195081	0.3630346	0.3601691	0.4061925	0.400932	0.432884	0.547336	0.592517	0.810671
Enthalpy Flow	kW	477.90234	-868.76725	59.588861	-5673.1308	-5673.130	-6636.3465	-6636.3467	-7194.9303	-8622.5044	-9022.3654	-10283.321
Average MW		32.066	28.652659	34.850985	34.850985	34.937170	34.937170	35.05818	35.05818	35.05818	35.05818	35.05818
Mole Flows	kmol/hr	129.1398	668.34982	668.30247	668.30247	666.65386	666.65386	664.3526	664.3526	664.3526	664.3526	664.3526
Mole Fractions												
H2O		0	0.0190165	0.0190179	0.0190179	0.0190648	0.0190648	0.019130	0.019130	0.0191305	0.0191305	0.0191305
H2SO4		0	0	8.53E-11	8.53E-11	7.19E-08	7.19E-08	4.41E-07	4.41E-07	4.41E-07	4.41E-07	4.41E-07
SO2		0	0	0.1930939	0.1930939	0.1886257	0.1886257	0.182352	0.182352	0.182352	0.182352	0.182352
SO3		0	0	0.0001417	0.0001417	0.0050877	0.0050877	0.012032	0.012032	0.012032	0.012032	0.012032
S		1	0	6.36E-46	6.36E-46	2.69E-51	2.69E-51	1.07E-52	1.07E-52	1.07E-52	1.07E-52	1.07E-52
N2		0	0.7728920	0.7729468	0.7729468	0.7748583	0.7748583	0.777542	0.777542	0.777542	0.777542	0.777542
O2		0	0.2080913	0.0147995	0.0147995	0.0123632	0.0123632	0.008942	0.008942	0.008942	0.008942	0.008942
Mass Flows	kg/hr	4141	19150	23291	23291	23291	23291	23291	23291	23291	23291	23291
Volume Flow	cum/hr	2.0562883	15863.400	106105.414	64156.402	64666.844	57339.806	58092.112	53804.201	42553.311	39308.519	28730.510

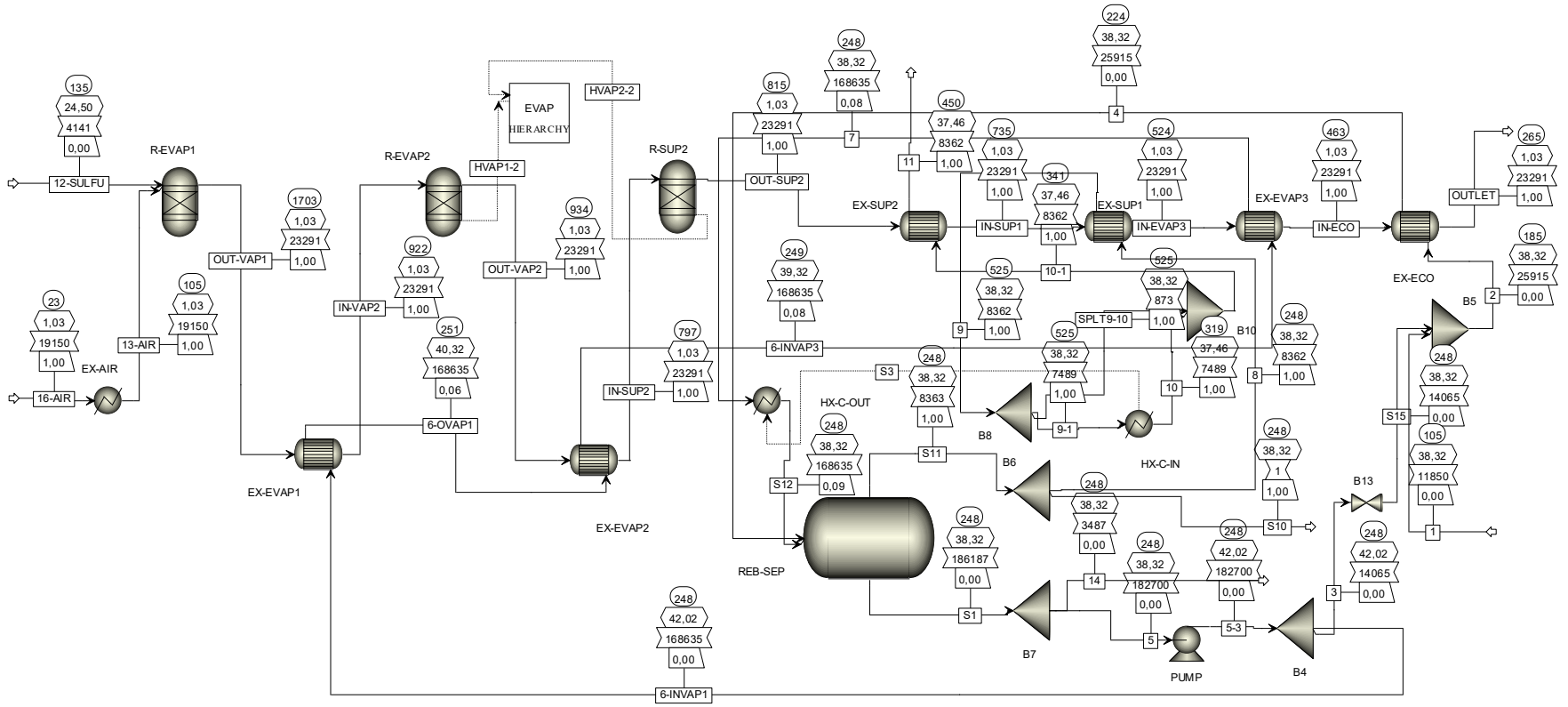

Figure 15-Simulation results for the sulfur dioxide production plant

8.2 Heat exchanger results

The temperature-duty (T-Q) diagrams of the heat recovery exchangers are presented in Figures 17 to 22. The results show a gradual decrease in the hot gas temperature from the evaporator to the superheater and economizer sections, confirming the recovery of a substantial amount of the thermal energy released in the unit.

In the first evaporator section, the maximum heat recovery load occurs at 1703 °C and drops to nearly 922 °C in Evaporator 1. The gas temperature at the outlet of Evaporator 2 is then decreased to 797 °C. The combustion gas is further cooled down to 734°C by superheater 2 in the cooling section, which also provides high-pressure steam. The next step is Superheater 1, where the temperature decreases to 524 °C.

Evaporator 3 decreases the temperature to 463 °C, and finally, the economizer with a large surface area provides substantial cooling, and it reduces the gas temperature to nearly 265 °C.

For all heat exchangers, the heat transfer surface areas were calculated and compared with the available technical documentation. For the heat exchangers equipped with finned or studded tubes, fin efficiencies were also considered in the calculations to obtain more realistic overall heat transfer coefficients and corrected heat transfer areas.

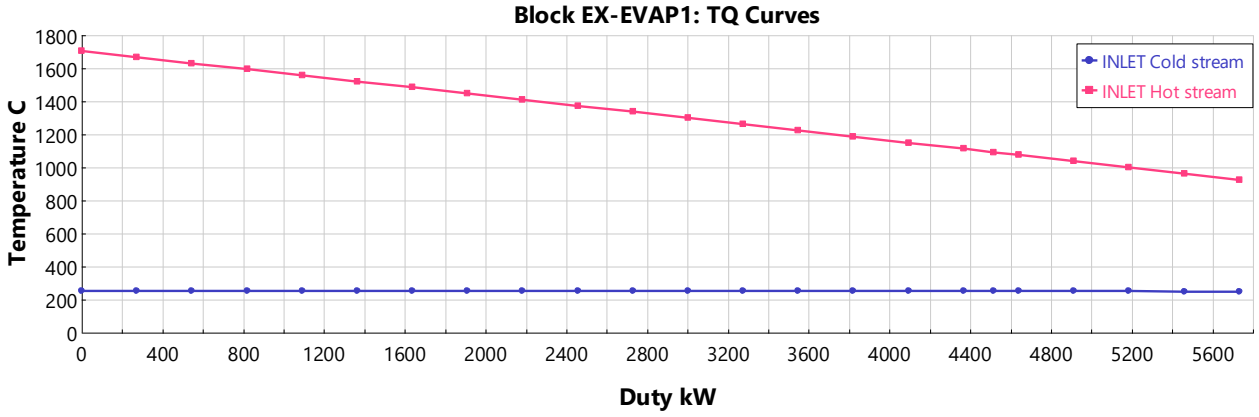

Figure 16-Evaporator 1 temperature vs duty curve

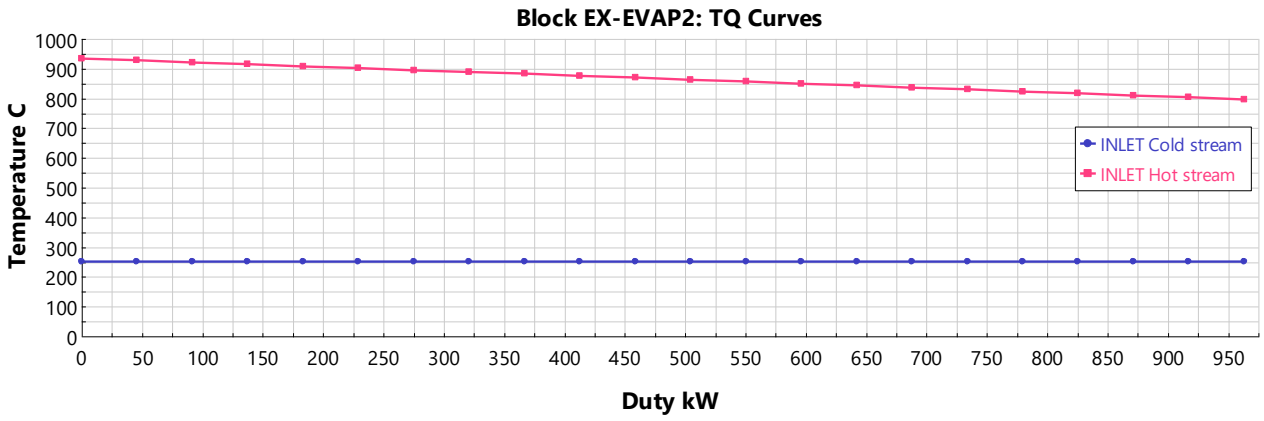

Figure 17-Evaporator 2 temperature vs duty curve

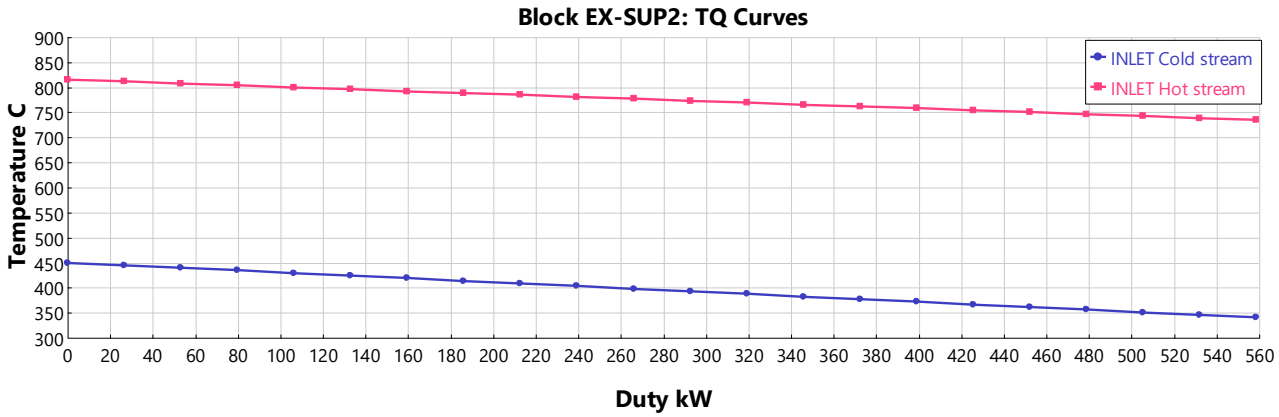

Figure 18-Super heater 2 temperature vs duty curve

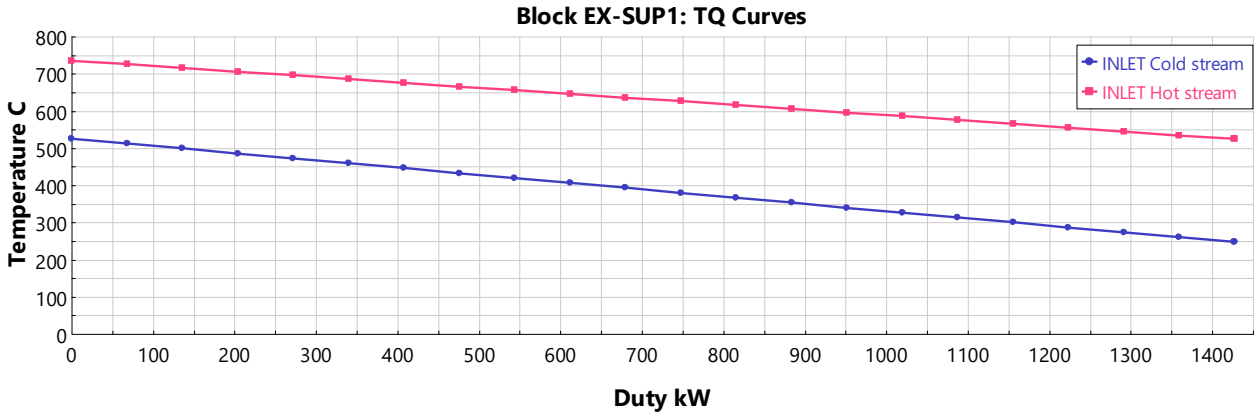

Figure 19-Super heater 1 temperature vs duty curve

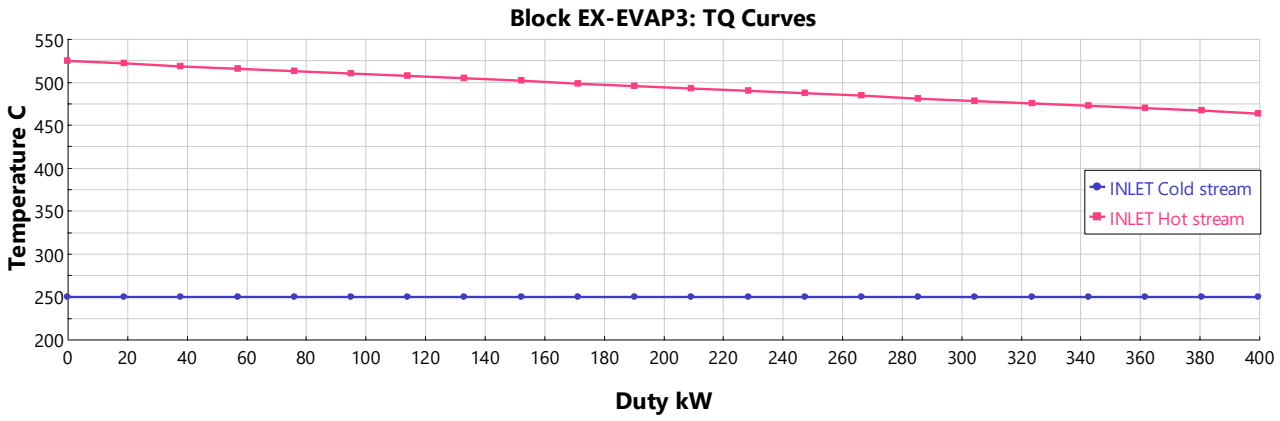

Figure 20-Evaporator 3 temperature vs duty curve

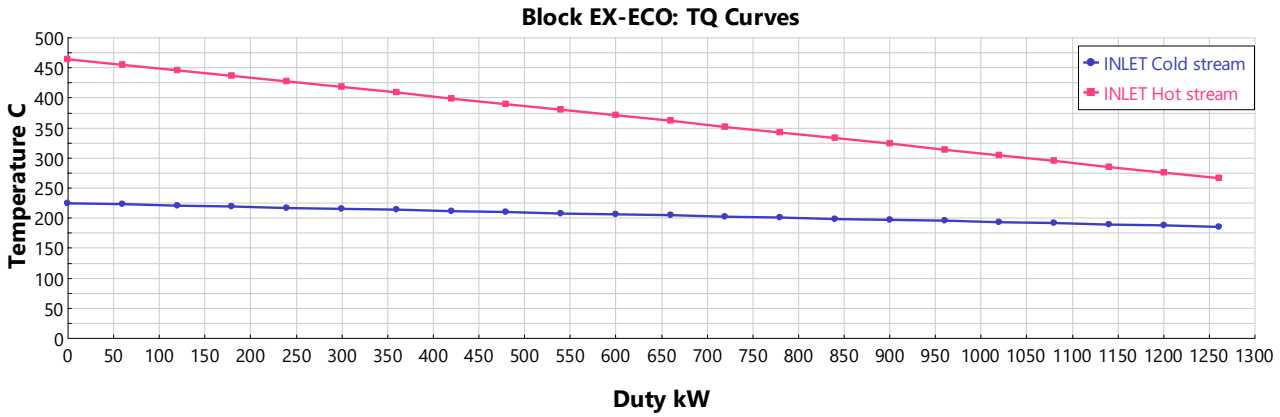

Figure 21-Economizer temperature vs duty curve

8.3 Sensitivity analysis results

8.3.1 Sensitivity analysis case 1

Sensitivity analysis case 1 was carried out to investigate the effect of inlet air humidity on sulfur trioxide formation, boiler temperature, sulfuric acid generation, and acid dew point temperature. The results show that the increase in air humidity causes significant

changes in the thermal behavior and the downstream acid formation during the cooling process.

As the inlet moisture flow rate increased from 0 to approximately 337 kg/h (corresponding to 0.02814 molar fraction of water vapor in the inlet air), the furnace outlet temperature decreased from nearly 1736 °C to about 1688 °C. This reduction is mainly related to the absorption of the generated heat by water vapor. At the same time, the sulfur dioxide concentration showed a slight decrease, while the sulfur trioxide concentration also decreased marginally throughout the studied range.

Results indicate that the sulfuric acid concentration increased by larger amounts of humidity in the inlet air. The H_2SO_4 mole fraction increased from negligible values to approximately 1.8×10^{-6} at the highest humidity level considered. This behavior is expected because additional humidity promotes sulfuric acid formation in the cooling sections of the process.

The results show that the sulfuric acid dew point temperature increases significantly with the increase in humidity. As the inlet moisture in the air increases, the calculated H_2SO_4 dew point Temperature increased from 190 °C to nearly 199 °C. This trend confirms that an increase in the humidity level increases the risk of acid condensation and corrosion in the downstream heat recovery equipment.

Table 12-Case 1 sensitivity analysis results

Humidity variation at inlet air KG/HR	YSO2*100	YSO3*100	BURNOUTT C	YH2SO4	H2SO4 acid dew point °C)
0	18.5901212	1.22753724	1736.09446	---	---
112.1	18.4148328	1.21530081	1719.674	6.10983E-07	189.6205204
186.8	18.2996219	1.20753399	1708.94196	1.01109E-06	193.7642702
228.96	18.2352159	1.20319606	1702.95594	1.23452E-06	195.4146156
298.9	18.1292088	1.19628366	1693.14173	1.60187E-06	197.5701716
336.3	18.0728599	1.19279545	1687.94971	1.79713E-06	198.5212615

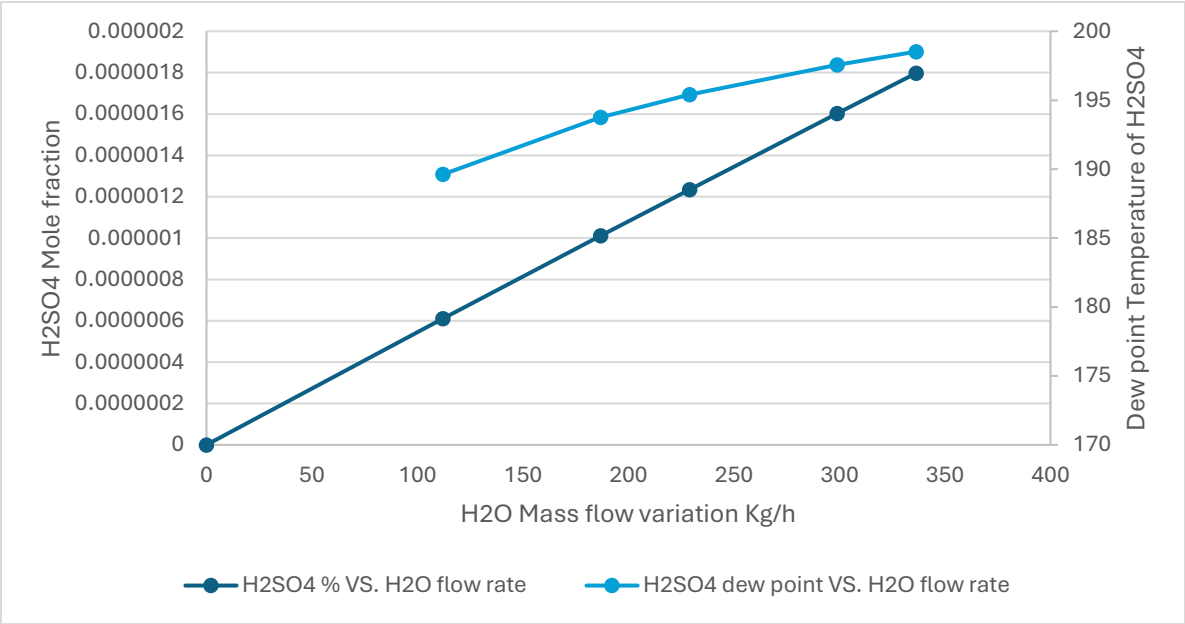

Figure 22-Case 1 sensitivity analysis plot

8.3.2 Sensitivity analysis case 2

Case 2 sensitivity analysis was performed to investigate the effect of inlet air temperature on the sulfur oxides formation, the furnace outlet temperature, and the sulfuric acid dew point behavior. The inlet air temperature was raised from 100 °C to 200 °C and changes in process performance, and the conditions for the formation of acids downstream were observed.

The results indicate that the furnace combustion temperature increases gradually with the increase in the inlet air temperature. The burnout temperature increased from approximately 1699 °C at 100 °C inlet air temperature to approximately 1772 °C at 200 °C. This is expected since the preheating of the combustion air requires less energy to heat the incoming reactants, thus allowing a larger fraction of the combustion heat to remain in the process gas.

Meanwhile, the sulfur dioxide concentration increased slightly with the increase of inlet air temperature, and the sulfur trioxide concentration decreased gradually. The reduction of SO_3 formation is because the SO_2 oxidation is an exothermic equilibrium, and at higher

temperatures, SO_2 is thermodynamically favored over SO_3. As a result, the concentration of the sulfuric acid was also gradually decreased in the temperature range investigated.

With increasing inlet air temperature, the calculated sulfuric acid dew point temperature decreased moderately from about 195.5 °C to almost 192.9 °C. This trend is directly related to the lower concentration of sulfuric acid formed at higher operating temperatures.

Table 13-Case 2 sensitivity analysis results

Inlet Air Temperature C	YSO2*100	YSO3*100	BURNOUTT C	YH2SO4	H2SO4 acid dew point °C
100	18.2256152	1.21382271	1699.2444	1.26E-06	195.5485206
105.1	18.2351285	1.20329278	1702.95594	1.23E-06	195.4158393
111.111111	18.2464153	1.19079968	1707.33241	1.21E-06	195.2570094
122.222222	18.2669464	1.1680744	1715.42781	1.15E-06	194.9640657
133.333333	18.2872199	1.1456342	1723.53149	1.11E-06	194.6695322
144.444444	18.3072348	1.12348014	1731.64425	1.06E-06	194.373426
155.555556	18.32699	1.10161359	1739.7669	1.01E-06	194.0757711
166.666667	18.3464845	1.08003544	1747.90025	9.70E-07	193.7765873
177.777778	18.3657178	1.05874652	1756.04504	9.28E-07	193.4758962
188.888889	18.3846891	1.03774748	1764.20201	8.89E-07	193.1737197
200	18.4033984	1.01703841	1772.37186	8.50E-07	192.8700737

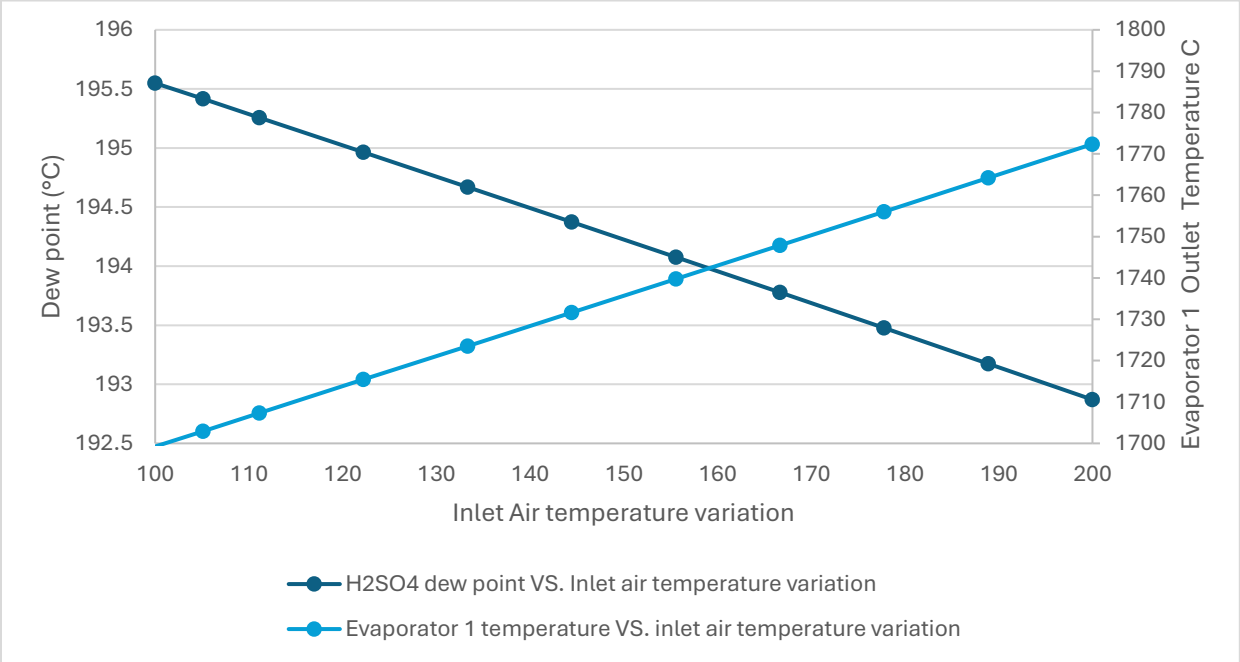

Figure 23-Case 2 sensitivity analysis plot

8.3.3 Sensitivity analysis case 3

This sensitivity analysis investigates the effect of an increasing oxygen concentration in the inlet air stream on the furnace temperature, sulfur dioxide concentration, and acid production. The oxygen mole fraction in the inlet stream increases from about 20.6% to 27.4% with an increase in inlet oxygen flow rate from about 4389 to 6389 kg/h. This influences on the reaction environment since more oxygen is available for the oxidation reactions.

The results indicate that the combustion outlet temperature gradually decreases from about 1707 °C to 1588 °C with the increase of oxygen availability. This is mainly due to the change in the gas composition and the heat absorption by the additional flow rate. Simultaneously, the SO_2 concentration is reduced from around 18.4 mol% to 15.4 mol% due to dilution, and the SO_3 concentration is increased from about 1.08 to 2.49 mol% in the outlet. This trend suggests that the further oxidation of SO_2 to SO_3 occurs with the increase of oxygen.

The sulfuric acid concentration increases slightly, from 1.14×10^{-6} to 1.90×10^{-6}, following the increase in SO_3 formation. As a result, the calculated H_2SO_4 acid dew point rises from about 193.8 °C to 206.1 °C.

Table 14-Case 3 sensitivity analysis results

Inlet air O2 mass flow KG/HR	YO2IN	YSO2*100	YSO3*100	BURNOUTT C	YH2SO4	O2 excess	H2SO4 acid dew point °C)
4389	0.20581411	18.4021428	1.08025883	1706.88874	1.14E-06	5.18%	193.8045107
4450.32385	0.20809138	18.2351764	1.20323968	1702.95594	1.23E-06	6.68%	195.4151675
4611.22222	0.21400473	17.864828	1.45231626	1692.72292	1.41E-06	10.63%	198.2347229
4833.44444	0.22202814	17.4455127	1.69773116	1678.80079	1.56E-06	16.10%	200.5711344
5055.66667	0.22988939	17.0861639	1.88084171	1665.12481	1.66E-06	21.57%	202.0915205
5277.88889	0.23759336	16.7642964	2.02651559	1651.69194	1.73E-06	27.05%	203.1856085
5500.11111	0.24514473	16.4686687	2.14713288	1638.49749	1.78E-06	32.55%	204.0212624
5722.33333	0.25254797	16.1927943	2.24979235	1625.53621	1.82E-06	38.05%	204.6852443
5944.55556	0.2598074	15.9327058	2.33879789	1612.80268	1.85E-06	43.56%	205.2267935
6166.77778	0.26692719	15.6851604	2.41764284	1600.29144	1.88E-06	49.07%	205.6809451
6389	0.27391131	15.4485766	2.487988	1587.99711	1.90E-06	54.60%	206.0656977

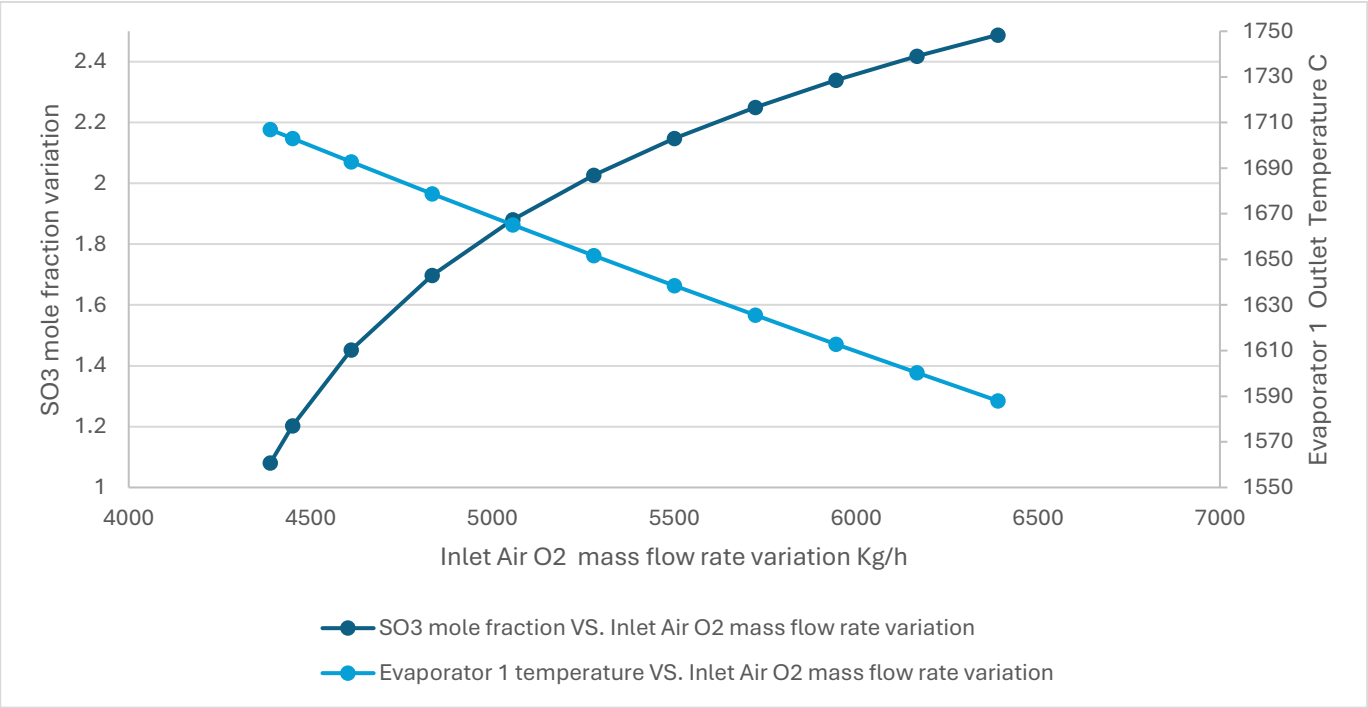

Figure 24-Case 3 sensitivity analysis plot

8.3.4 Sensitivity analysis case 4

The fourth sensitivity analysis examines the effect of different inlet air flow rates on sulfur oxide formation, furnace temperature, oxygen excess, and acid dew point behavior. The inlet air flow rate varied from 18,000 to 23,000 kg/h.

It is found that with increasing the inlet air flow rate, more oxygen goes into the combustion system, leading to an increase in the excess oxygen concentration at the outlet from about 0% to about 28 mol%. Simultaneously, the concentration of sulfur dioxide drops from about 20.2 mol% to almost 14.3 mol% due to dilution of the gas.

The sulfur trioxide concentration increases gradually with increasing air flow rate from about 0.40 mol% to nearly 1.89 mol%. The higher oxygen availability favors the oxidation of sulfur dioxide according to the reversible exothermic equilibrium reaction between SO_2 and SO_3. Consequently, the concentration of sulfuric acid also increases progressively over the range studied.

The results show a continuous increase in the sulfuric acid dew point temperature, from about 179 °C at low oxygen excess conditions, to 202 °C at the highest air flow rate considered. This increase is directly related to larger amounts of SO_3 and sulfuric acid produced in the process gas.

Moreover, the increase in air flow rate leads to a decrease in the boiler outlet temperature from about 1787 °C to near 1476 °C. This trend is mainly caused by the lack of thermal load to heat the larger quantity of inlet air entering the boiler.

Table 15-Case 4 sensitivity analysis results

Air flow KG/HR	YO2*100	YSO2*100	YSO3*100	YH2O*100	BURNOUTTC	YH2SO4	O2 excess	pSO3 (atm)	pH2O (atm)	H2SO4 acid dew point °C)
18000	0.054924347	20.2013127	0.396059071	1.9054045	1787.10488	4.74E-07	-0.04%	0.004045607	0.019463051	179.102855
18250	0.19577814	19.6638398	0.680170476	1.90809569	1768.03405	7.67E-07	1.34%	0.006947707	0.019490541	186.89369
18500	0.373114687	19.2118426	0.876919647	1.90996004	1749.40497	9.52E-07	2.73%	0.008957432	0.019509584	190.6495115
18750	0.567634964	18.8103673	1.02516912	1.91136512	1731.20748	1.08E-06	4.12%	0.01047175	0.019523937	192.9899371
19000	0.770519139	18.4430511	1.14295796	1.91248165	1713.42831	1.18E-06	5.51%	0.011674922	0.019535342	194.634034
19150	0.894256524	18.2352046	1.20320847	1.91305281	1702.95594	1.23E-06	6.34%	0.01229036	0.019541176	195.4147726
19250	0.97719616	18.1010886	1.23986808	1.91340034	1696.05386	1.27E-06	6.90%	0.012664826	0.019544726	195.872155
19500	1.18493771	17.7789592	1.32180844	1.91417714	1679.07075	1.33E-06	8.29%	0.013501818	0.019552661	196.850505
19750	1.39211642	17.4731242	1.39247971	1.9148471	1662.46605	1.39E-06	9.67%	0.014223701	0.019559504	197.6499004
20000	1.59767577	17.1810821	1.45443056	1.91543437	1646.2273	1.45E-06	11.06%	0.014856508	0.019565503	198.3201348
20250	1.80091891	16.9009956	1.50947638	1.91595615	1630.34252	1.50E-06	12.45%	0.015418782	0.019570833	198.8937038
20500	2.00138162	16.6314654	1.55895197	1.91642509	1614.80028	1.54E-06	13.84%	0.015924158	0.019575623	199.3928362
20750	2.19875727	16.3713973	1.60386086	1.9168507	1599.58957	1.59E-06	15.23%	0.016382887	0.01957997	199.8332801
21000	2.39283746	16.1198944	1.64499472	1.91724048	1584.6999	1.63E-06	16.61%	0.016803055	0.019583952	200.2267332
21250	2.58349685	15.8762314	1.68296305	1.9176002	1570.12117	1.67E-06	18.00%	0.017190888	0.019587626	200.5818567
21500	2.77066145	15.6397956	1.71825765	1.91793455	1555.84373	1.71E-06	19.39%	0.01755141	0.019591041	200.9053425
21750	2.95429654	15.4100654	1.75127711	1.91824728	1541.85834	1.75E-06	20.78%	0.017888693	0.019594236	201.2024213
22000	3.13439624	15.1865903	1.78234827	1.9185415	1528.15612	1.79E-06	22.17%	0.018206074	0.019597241	201.4772454
22250	3.31097194	14.9689692	1.81175036	1.91881986	1514.72858	1.83E-06	23.56%	0.018506406	0.019600084	201.7332289
22500	3.48406282	14.7568699	1.83969321	1.91908435	1501.56754	1.86E-06	24.94%	0.018791833	0.019602786	201.9729481
22750	3.65370833	14.5499767	1.86637471	1.91933685	1488.66519	1.90E-06	26.33%	0.019064375	0.019605365	202.1987031
23000	3.81996031	14.3480128	1.8919561	1.91957887	1476.01402	1.94E-06	27.72%	0.01932568	0.019607837	202.4123461

8.3.5 Sensitivity analysis case 5

In the case 5 sensitivity analysis, the sulfur feed flow rate was varied from 3500 to 6000 kg/h (as the design case). The inlet air flow rate was adjusted with the sulfur feed using an air-to-sulfur ratio of 5.05. This case varies from the operating case, where the sulfur flow rate is 4141 kg/h, and the air flow rate is 19150 kg/h, corresponding to a lower air-to-sulfur ratio of about 4.6. The sulfur flow rate directly increases the heat released in the furnace. Therefore, the cooling-side conditions also had to be adjusted during the sensitivity study. If only the sulfur flow rate were changed while keeping the separator pressure and water circulation fixed, the cooling fluid would dry out in the evaporator section. For this reason, the separator pressure, make-up water flow rate, and circulation flow rate were increased as the sulfur feed increased, to maintain a stable vapor fraction in the separator and avoid complete evaporation of the cooling stream.

The results show that increasing the sulfur feed increases both the heat release in the furnace and the thermal load of the recovery section. The high-pressure steam production increased from 10,425 kg/h at 3500 kg/h sulfur to 15,925 kg/h at 6000 kg/h sulfur. At the same time, the make-up water required increased from 10,750 to 16,250 kg/h, while the separator circulation flow increased from 105,785 to 161,595 kg/h. The difference of 325 kg/h between make-up water and high-pressure steam is due to the liquid outlet to the outside of this plant. The separator pressure also increased from 37.25 to 42.6 bar. These changes show that higher sulfur throughput requires a stronger cooling and circulation system to keep the water/steam side stable.

About the temperature profile, as the sulfur feed rate increased, the outlet temperatures of the exchangers increased because more combustion and heat occurred inside the furnace. The gas temperature leaving Evaporator 1 increased from 822 °C to 1073 °C. The outlet gas temperature leaving the economizer increased from 244 °C to 386 °C. The heat duties of all exchangers also increased with an increase in sulfur flow rate. The duty of Evaporator 1 increased from 5113.57 kW to 5958.31 kW, and the economizer duty increased from 989.28 kW to 2434.24 kW, which confirms that a higher sulfur flow rate increases the recoverable heat in the system.

The increase of the sulfur flow rate from 3500 kg/h to 6000 kg/h led to an increase of the SO_2 concentration with the increase of the sulfur flow rate from 0.1529 kg/h to 0.1722 kg/h. This behavior is reasonable because higher sulfur feed results in higher combustion temperatures, and the oxidation of SO_2 to SO_3 is an exothermic equilibrium reaction. At higher temperatures, SO_3 formation becomes less favorable, so more sulfur dioxide remains as SO_2. As a result, the amount of H_2SO_4 in the product also decreased from $1.66 \times 10^{-6}$to 5.18×10^{-8}.

This change in acid formation had a large effect on the acid dew point. At the lowest sulfur feed rate, the H_2SO_4 acid dew point was approximately 207.66 °C, which decreased to approximately 182.50 °C at 6000 kg/h. This is important for heat recovery because the lower acid dew point allows the gas to be cooled further before sulfuric acid condensation becomes a corrosion concern. The available heat recovery above the dew point temperature thus increased from approximately 201 kW at 3500 kg/h sulfur to nearly 1988 kW at 6000 kg/h sulfur.

For the operating case with a sulfur feed rate of 4141 kg/h, the total duty recovered through the heat exchanger network in Aspen Plus was approximately 10.37 MW, while the overall furnace energy balance reached about 11.18 MW. This shows that most of the thermal energy released during sulfur combustion was effectively recovered through the waste heat boiler system and associated exchangers. The remaining difference is mainly related to unrecovered heat leaving with the process gas, together with minor thermal losses within the system. Overall, the results indicate that the current heat recovery arrangement utilizes a large portion of the available combustion energy and provides a proper thermal integration across the process.

Table 16-Case 5 sensitivity analysis concentration results

S	Air	Separator Circulation kg/h	Separator Pressure bar	Separator Vapor fraction	Inlet water kg/h	High pressure steam Kg/h	H2O in product mol fraction	SO2 in product mol fraction	SO3 in product mol fraction	H2SO4 in product mol fraction	YSO2*100	YSO3*100	YH2O*100
6000	30320	161595	42.6	0.0985	16250	15925	0.01906427	0.17224469	0.00502384	5.18E-08	17.22446907	0.502384438	1.90642702
5500	27793	150433	41.53	0.0985	15150	14825	0.019078804	0.17085009	0.006556	8.73E-08	17.08500947	0.65560035	1.90788038
5000	25250	139271	40.46	0.0985	14050	13725	0.019100656	0.16886339	0.0088616	1.59E-07	16.88633934	0.886159996	1.9100656
4500	22725	128109	39.39	0.0985	12950	12625	0.019134565	0.16559767	0.01244416	3.19E-07	16.55976713	1.244415535	1.91345647
4000	20200	116947	38.32	0.0985	11850	11525	0.019186906	0.16054419	0.0179878	6.99E-07	16.05441927	1.79878046	1.91869062
3500	17675	105785	37.25	0.0985	10750	10425	0.019265314	0.15293685	0.02633272	1.66E-06	15.29368488	2.633271871	1.92653142
4141	19150	116947	38.32	0.0985	11850	11525	0.019129767	0.18242532	0.01195099	4.31E-07	18.24253178	1.195098546	1.91297668

Table 17-Case 5 sensitivity analysis temperature results

S	R-2502A Temp C	EX-EVAP1 Temp C	R-2502B Temp C	EX-EVAP2 Temp C	R-2503B Temp C	EX-SUP2 Temp C	EX-SUP1 Temp C	EX-EVAP3 Temp C	EX-ECO Temp C
6000	1589	1073	1079	972	978	908	683	622	386
5500	1589	1036	1044	932	940	869	643	582	355
5000	1590	994	1004	888	899	827	601	542	324
4500	1590	946	960	838	855	782	558	500	295
4000	1590	889	909	782	807	735	513	457	268
3500	1590	822	854	722	757	686	468	415	244
4141	1703	922	935	798	815	738	507	450	261

Table 18-Case 5 sensitivity analysis duty results

S	EX-EVAP1 Duty kW	EX-EVAP2 Duty kW	EX-SUP2 Duty kW	EX-SUP1 Duty kW	EX-EVAP3 Duty kW	EX-ECO Duty kW
6000	5958.313	1206.84	783.647	2463.81	650.332	2434.24
5500	5842.96	1149.946	727.373	2252.37	588.142	2138.91

5000	5709.82	1086.061	665.746	2030.9	522.701	1840.23
4500	5547.913	1013.715	598.722	1802.042	454.702	1545.672
4000	5352.836	932.58	526.906	1569.28	385.712	1259.76
3500	5113.57	843.094	450.735	1336.12	316.592	989.277
4141	5728.932	964.074	536.152	1563.23	374.661	1199.36

Table 19-Case 5 sensitivity analysis acid dew point results

S	pSO3 (atm)	pH2O (atm)	H2SO4 acid dew point °C)	pSO2 (mmHg)	pH2O (mmHg)	H2SO3 acid dew point (°C)	Heat Recovery to Dew Point kW
6000	0.005132	0.0194735	182.4955088	133.7159375	14.79985681	16.00167568	1988.22
5500	0.006697	0.01948834	186.3550507	132.6332934	14.8111395	16.0143449	1501.028
5000	0.009052	0.01951066	190.8058993	131.0909896	14.82810363	16.03331075	1078.276
4500	0.012711	0.0195453	195.9280673	128.5557643	14.85442741	16.06289441	719.289
4000	0.018374	0.01959876	201.6207618	124.632679	14.89506083	16.10860162	424.754
3500	0.026898	0.01967886	207.6633713	118.7269926	14.95593011	16.17719503	201.14
4141	0.012208	0.0195404	195.3118388	141.6192993	14.85070277	16.04615833	399.826

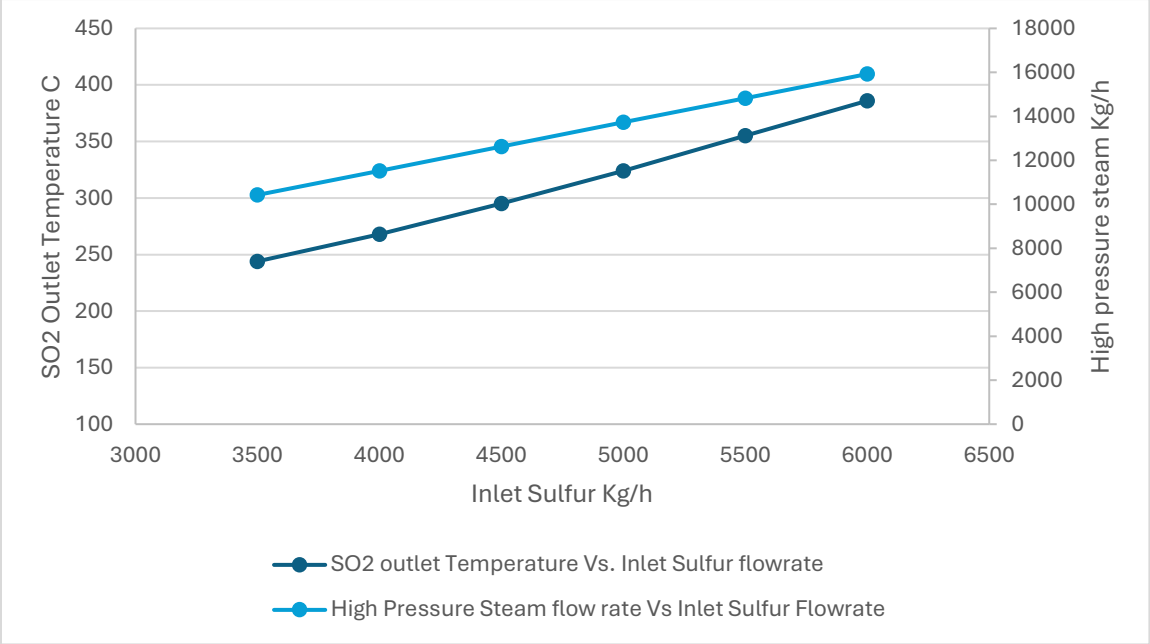

Figure 25-Case 5 sensitivity analysis plot 1

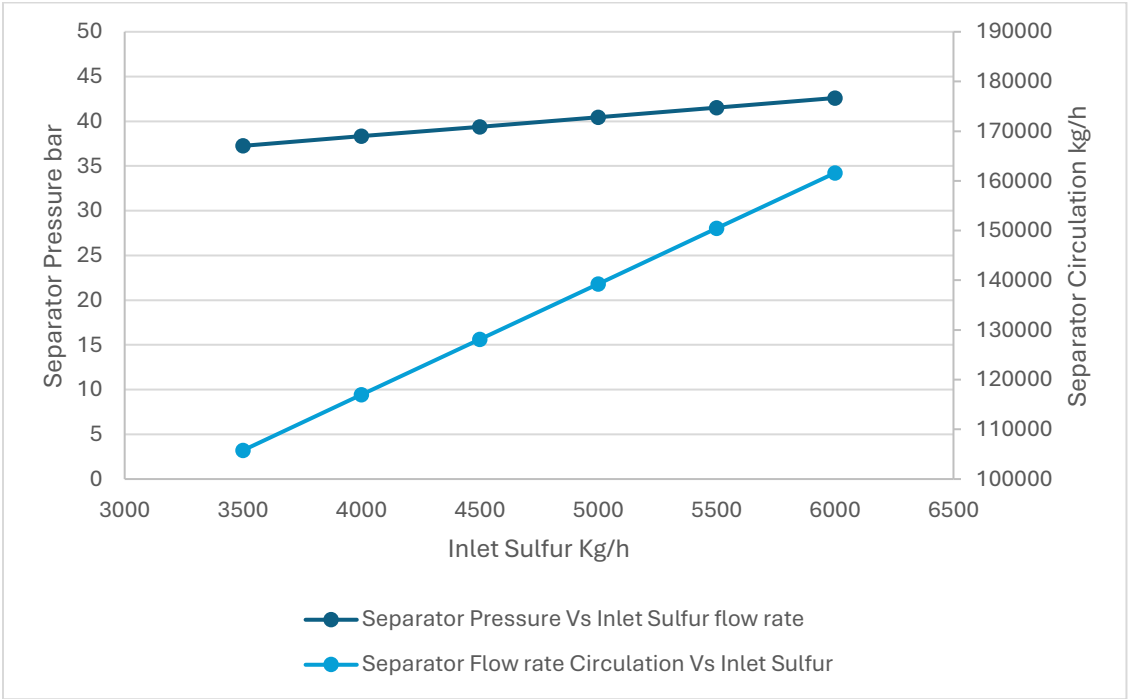

Figure 26-Case 5 sensitivity analysis plot 2

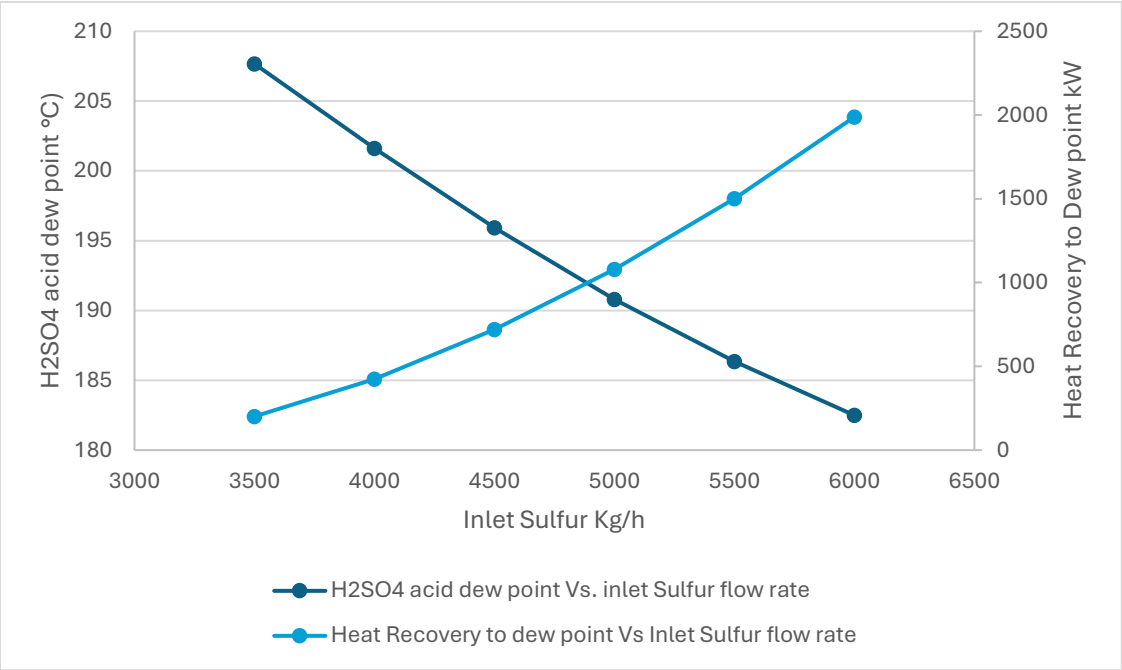

Figure 27-Case 5 sensitivity analysis plot 3

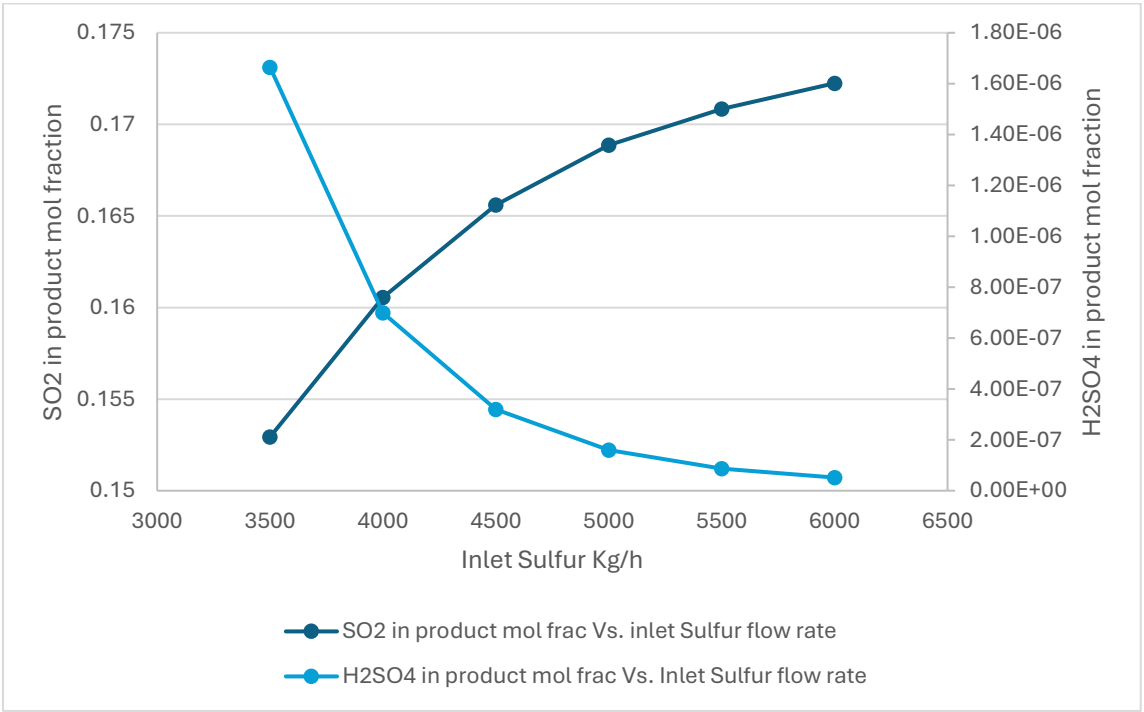

Figure 28-Case 5 sensitivity analysis plot 4

8.4. Energy analysis, heat recovery, and pinch technology results

This section represents energy analysis and pinch technology results. Stream data used in Aspen Energy Analyzer are mentioned in Table 20, which can be used to generate composite curve and grand composite curve to implement energy analysis in the plant.

Table 20-Aspen energy analyzer input data

Name		Inlet T [C]	Outlet T [C]	MCp [kJ/C-h]	Enthalpy [kJ/h]	Segm.	HTC [kJ/h-m2-C]	Flowrate [kg/h]	Effective Cp [kJ/kg-C]	DT Cont. [C]
EX-AIR		22,0	100,0	2,079e+004	1,622e+006		720,00	—	—	Global
EX-EVAP1-HOT		1703,0	922,0	2,642e+004	2,064e+007		5853,24	—	—	Global
EX-EVAP2-HOT		934,0	797,0	2,531e+004	3,468e+006		5853,24	—	—	Global
EX-SUP2-HOT		815,0	735,0	2,514e+004	2,011e+006		5853,24	—	—	Global
EX-SUP1-HOT		735,0	524,0	2,436e+004	5,139e+006		5853,24	—	—	Global
EX-EVAP3-HOT		524,0	463,0	2,360e+004	1,439e+006		5853,24	—	—	Global
EX-ECO-HOT		463,0	265,0	2,293e+004	4,539e+006		5853,24	—	—	Global
EX-EVAP1-COLD		248,0	251,0	6,879e+006	2,064e+007		21600,00	—	—	Global
EX-EVAP2-COLD		248,0	249,0	3,468e+006	3,468e+006		21600,00	—	—	Global
EX-SUP2-COLD		341,0	450,0	1,845e+004	2,011e+006		21600,00	—	—	Global
EX-SUP1-COLD		248,0	525,0	1,855e+004	5,139e+006		21600,00	—	—	Global
EX-EVAP3-COLD		249,0	250,0	1,439e+006	1,439e+006		21600,00	—	—	Global
EX-ECO-COLD		185,0	224,0	1,164e+005	4,539e+006		9198,36	—	—	Global
EX-REC		265,0	205,0	2,703e+004	1,622e+006		836,22	—	—	Global

8.4.1 Composite curve

The composite curves generated in Aspen Energy Analyzer show that a large amount of heat is available from the sulfur combustion gas over a very wide temperature range, extending from approximately 1703 °C down to the final gas cooling section near 265 °C. An extra cooling heat exchanger was considered for the heat recovery of the gas from 265 °C to 205 °C, which is the highest sulfuric acid dew point temperature among sensitivity analysis scenarios. The hot composite curve decreases continuously, indicating progressive sensible heat recovery throughout the waste heat boiler train.

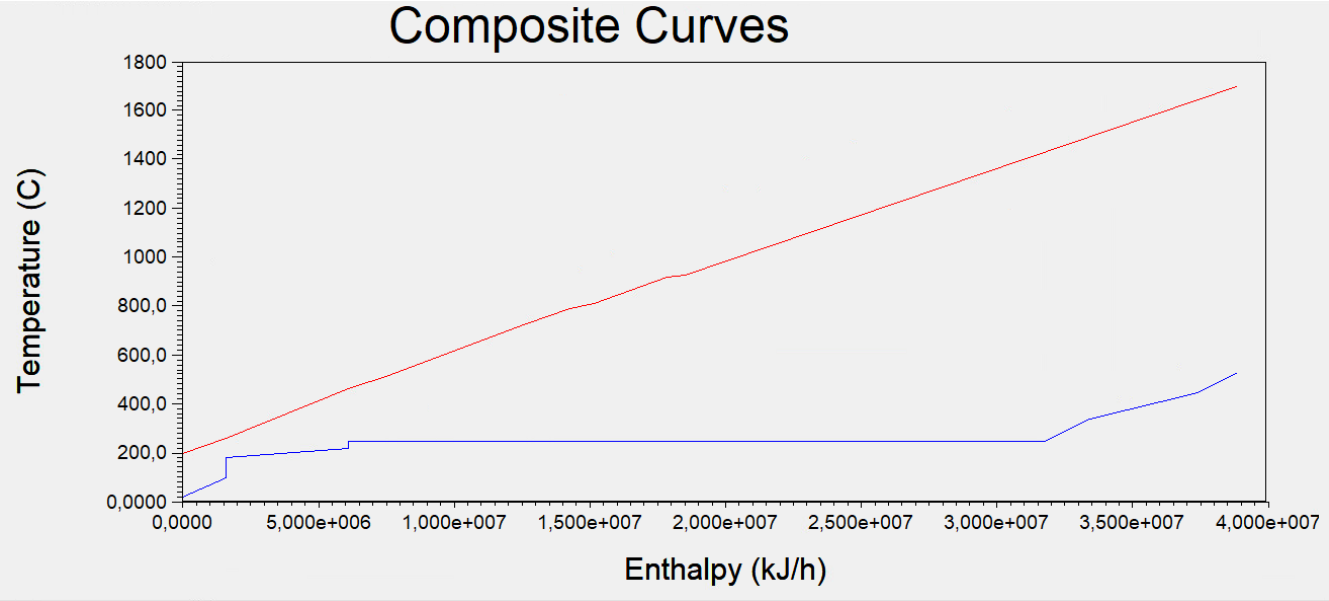

Figure 29-Composite curve

The cold composite curve shows three main regions:

1. Low-temperature heating region

   This region corresponds mainly to feed-water heating and air preheating.

2. Evaporation region

   Around 248–251 °C, the cold composite curve becomes nearly horizontal. This behavior corresponds to steam generation inside the evaporators, where a large latent heat load is absorbed while temperature changes only slightly.

3. Superheating region

   Between approximately 341 °C and 525 °C, the cold composite curve rises again due to steam superheating before the steam enters the turbine section at 450 °C.

The Aspen composite curve indicates that the closest temperature approach in the current exchanger network occurs mainly at the end of the cooling stage. The composite curves indicate a relatively narrow approach in the economizer region. In the economizer, the hot gas is cooled from approximately 463 °C to 265 °C while the feed water is heated from approximately 185 °C to 224 °C. In this section, the hot gas temperature approaches approximately 265 °C while the steam temperature reaches approximately 185 °C:

$$\Delta T = 265 - 185 = 80^{\circ}C \qquad (8.1)$$

This region represents the main practical pinch location in the heat recovery system according to the Pinch technology.

After the pinch analysis, the existing heat recovery network was also plotted as a temperature–heat load profile (T vs. Q) in order to compare the ideal pinch target with the actual exchanger arrangement. Unlike the composite curves, Figure 32 follows the real sequence of exchangers in the process and therefore shows the actual temperature approach in each heat recovery unit. The result indicates that the most important temperature approach occurs in the superheater region, where the hot gas temperature decreases toward about 525 °C while the cooling steam temperature reaches approximately 524 °C in HX-SUP1 and finally leaves as superheated steam at 450 °C in EX-SUP1.

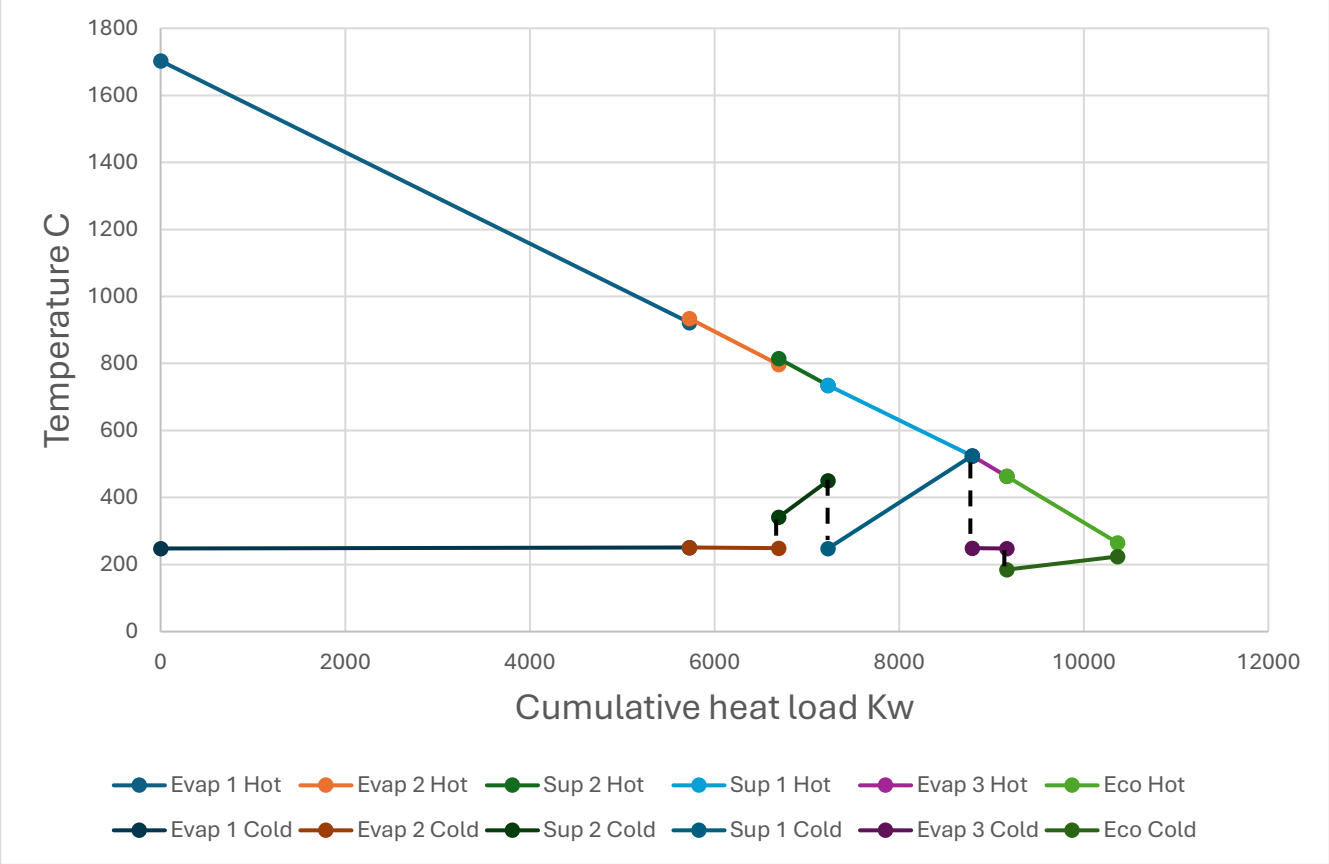

Figure 30-Temperature VS. cumulative heat load

The superheater sections are critical because the recovered heat is used to superheat the generated steam before it is sent to the turbine. Therefore, although the Aspen Energy Analyzer composite curves provide the thermodynamic heat recovery target, the actual process T–Q profile shows that the main practical constraint of the existing exchanger network is located around the superheater section. The final low-temperature section in the economizer remains as both the sulfuric acid dew point and the classical pinch limitation.

8.4.2 Grand composite curve

The Grand composite curve (GCC) provides the net heat surplus and deficit in the process temperature range. The GCC generated by Aspen Energy Analyzer shows a large heat surplus at high temperatures due to sulfur combustion. As the temperature decreases, the available heat is progressively consumed by steam generation, superheating, economizer heating, and finally air preheating.

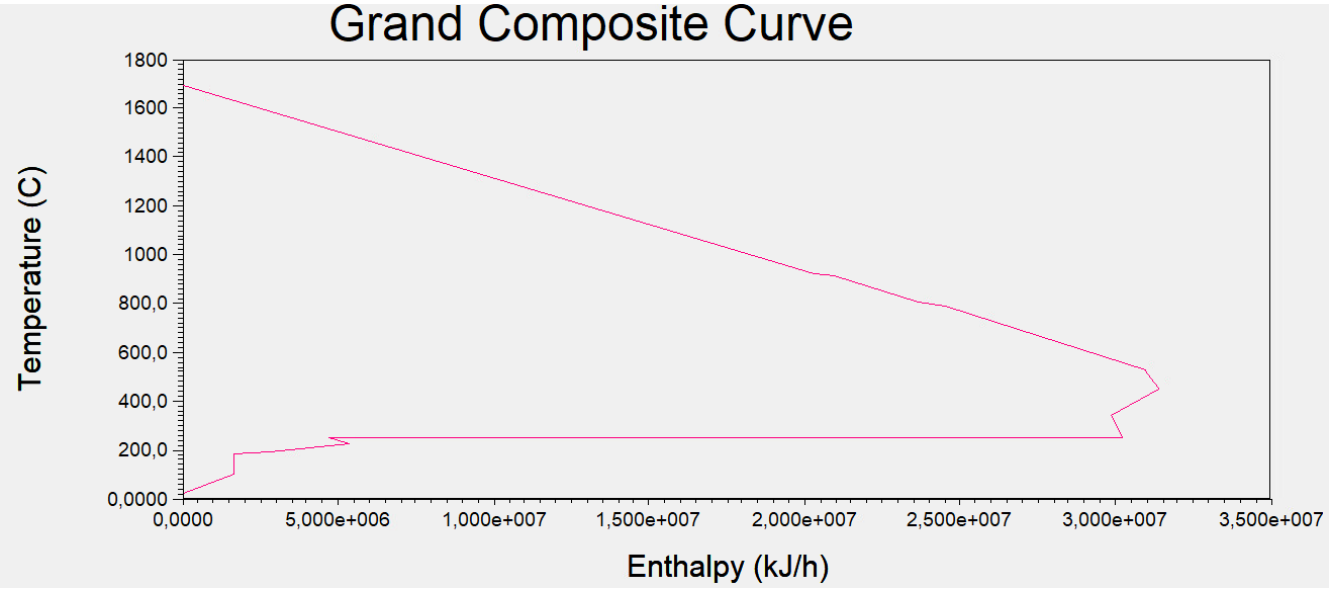

Figure 31- Grand composite curve

A pronounced transition appears around the evaporation temperature region because a large amount of latent heat is transferred at nearly constant temperature. This produces the characteristic sharp section visible on the GCC.

The middle section of the GCC corresponds to the superheater region. In this region, the heat-capacity rates of the hot and cold streams become relatively close, producing the minimum temperature approach observed in the network. This confirms that the primary pinch occurs around the superheater section at 450 C.

The GCC also shows a secondary narrowing tendency in the economizer region before the final gas cooling section. This behavior corresponds to the reduced remaining driving force after most of the high-temperature heat has already been recovered in the upstream exchangers. Nevertheless, the economizer approach remains acceptable because the final limitation in this region is the sulfuric acid dew point rather than insufficient thermal driving force.

At low temperatures, the GCC still shows remaining heat recovery potential between approximately 265 °C and the sulfuric acid dew point region. However, further cooling of the process gas below approximately 205 °C is not acceptable because sulfuric acid condensation may occur, leading to severe corrosion problems.

8.4.3 Thermal oil loop sensitivity analysis with sulfur flow rate

During the sulfur-flow sensitivity analysis, the sulfur feed was increased from 3500 to 6000 kg/h. As sulfur flow increased, the final SO_2-rich gas temperature increased from approximately 261 °C to 386 °C, while the sulfuric acid dew point increased from approximately 182 °C to 207 °C. Therefore, the thermal oil system must operate safely over a wider temperature range. As an example, Therminol 66 oil was considered for oil loop calculations. Considering the cp value equals 2.4 (kj/kg.K), it is possible to provide a sensitivity analysis.

Table 21-Thermal oil loop sensitivity analysis

Sulfur flow (kg/h)	Heat recovery (kW)	Oil flowrate, ΔT=50°C (kg/s)	Oil flowrate, ΔT=30°C (kg/s)
3500	201	1.68	2.79
4000	425	3.54	5.9
4500	719	5.99	9.99
5000	1078	8.99	14.98
5500	1501	12.51	20.85
6000	1988	16.57	27.61

The table shows that increasing sulfur feed significantly increases the required oil circulation rate. The same oil may still be used throughout the operating range, but the circulation flow rate must increase accordingly to maintain acceptable oil temperatures.

At the highest sulfur-load case, the gas temperature approaches approximately 386 °C. Therefore, the thermal stability of the selected oil becomes critical. Increasing the oil circulation rate helps reduce local film temperatures and improves temperature control, but the selected oil must still tolerate the highest gas-side temperature exposure.

Table 22-Thermal oils candidates

Oil type	Cp (kJ/kg·K)	Maximum operating range	Suitability
Therminol 66 [43]	2.3–2.5	bulk 345 °C, film 375 °C	Best practical choice
Dowtherm A / VP-1 [44]	2.0–2.2	up to 400 °C	Safest option for the highest sulfur-load case
Dowtherm T [45]	2.3–2.5	optimum 288 °C, extended 315 °C	Suitable for moderate-temperature operation
Mobiltherm 603 [46]	2.4–2.6	approximately 285 °C	Suitable for lower sulfur-flow conditions
Mobiltherm 605 [46]	2.4–2.6	approximately 315 °C	Better than Mobiltherm 603 for elevated temperatures

For the base operating condition, Therminol 66 can be suitable because the bulk oil temperature remains in the recommended operating range. However, for the 6000 kg/h sulfur case, the gas-side temperature approaches the film-temperature limitation of Therminol 66. Under these conditions, either a higher circulation flow rate should be used to reduce local oil-film temperatures, or a more thermally stable fluid, such as Dowtherm A, should be selected.

9. Conclusion

In this work, the simulation and analysis of a sulfur dioxide production and heat recovery process with the use of Aspen Plus were presented. The thermal behavior of the sulfur combustion section, sulfur dioxide formation, heat recovery performance, and the effect of several operating variables on the overall process conditions were the focus of the study. A complete steady-state process model was developed with the use of the ELECNRTL property method to represent the behavior of sulfur oxides, water vapor, and sulfuric acid formation throughout the unit.

The simulation results indicate that sulfur combustion generates a high-temperature gas stream with a high concentration of sulfur dioxide and a combustion temperature of 1700 °C. The recovered thermal energy was efficiently achieved in a train of evaporator, superheater, and economizer exchangers, resulting in significant steam generation and heat recovery within the process. Due to the existence of humidity in the inlet air, the risk of sulfuric acid formation was considered, and the outlet furnace temperature was maintained above the sulfuric acid dew point temperature to minimize the risk of acid condensation and downstream corrosion.

Emphasis was laid on the heat recovery section and calculations for the exchanger. The heat transfer areas were assessed and compared to the available process documentation. For exchangers with finned tubes, corrections for fin efficiency were considered in the calculations to obtain more realistic overall heat transfer coefficients and effective heat transfer areas. The consistency between the exchanger thermal performance and the operating process conditions obtained from the simulation was improved with this approach.

The effects of inlet humidity, inlet air temperature, oxygen concentration, air flow rate, and sulfur feed rate on sulfur oxide formation and process behavior were evaluated through several sensitivity analyses. The results showed that a rise in humidity favors the formation of sulfuric acid, as well as enhances the acid dew point temperature, which could lead to an increase in the corrosion tendency in low-temperature equipment. In contrast, increasing inlet air temperature reduced SO_3 and H_2SO_4 formation due to the temperature dependence of the SO_2 oxidation equilibrium reaction. The analyses also

showed that excess oxygen favors the formation of SO_3. This leads to higher sulfuric acid concentrations and increasing acid dew point temperatures.

Sensitivity analysis of the sulfur flow rate indicates that higher sulfur throughput improves sulfur dioxide production, steam generation and heat recovery potential. At higher sulfur flow rates, the combustion temperature increased, and the formation of SO_3 and sulfuric acid became less favorable. As a result, the sulfuric acid dew point temperature decreased while the available heat recovery above the dew point increased significantly.

The study also showed that the cooling and circulation system cannot remain fixed when sulfur throughput changes, since separator pressure, make-up water flow, and circulation flow rate must be adjusted to maintain stable evaporator operation and prevent dry-out conditions.

Overall, the developed process model provided a realistic representation of the sulfur combustion and heat recovery system and allowed the interaction between reaction behavior, thermal recovery, and acid formation to be evaluated under different operating conditions. The results obtained in this work may be useful for further process optimization, energy integration studies and future research on sulfur oxide recovery and corrosion control in industrial sulfur processing systems.

References

[1] H. Müller, “Sulfur Dioxide” Ullmann’s Encyclopedia of Industrial Chemistry, Wiley-VCH. doi: 10.1002/14356007.a25_569., 2012.

[2] A. M. e. al., "Dynamic Modeling and Simulation of the Sulfur Combustion Furnace in Industrial Smelter," *Processes,* Vols. 10, no. 12, p. 2655, 2022.

[3] M. R. Z. e. al., "Modelling and Multi-Objective Optimization of the Sulphur Dioxide Oxidation Process," *Processes,* Vols. 9, no. 6, p. 1072, 2021.

[4] H. P. a. T. M. L. W. S. J. Smith, ""“Global and Regional Anthropogenic Sulfur Dioxide Emissions," *Global Environmental Change,,* Vols. 11, no. 1, p. 73–83, 2001.

[5] P. G. e. al., ""“Acid Rain and Air Pollution: 50 Years of Progress in Environmental Science and Policy,”," *Ambio,* vol. 49, p. 849–864, 2020.

[6] K. A. F. J. a. B. L. D. Fleig, ""“Measurement and Modeling of Sulfur Trioxide Formation in a Pressurized Oxy-Fuel Flame,”," *Combustion and Flame,* Vols. 160, no. 12, p. 2849–2863, 2013.

[7] N. G. A. a. K. R. Golwalkar, "A Practical Guide to the Manufacture of Sulfuric Acid, Oleums, and Sulfonating Agents," *Springer,* 2013.

[8] K. A. F. J. a. B. L. D. Fleig, "Measurement and Modeling of Sulfur Trioxide Formation in Combustion Systems," *Combustion and Flame,* vol. 160, no. 12, p. 2849–2863, 2013.

[9] H. X. e. al., "Experimental Study of SO_3 Formation in Combustion Systems," *Aerosol and Air Quality Research,* 2018.

[10] J. T. B. F. H. Verhoff, "Predicting dew point of gases," *Chemical engineering Progress,* no. 78 (8), pp. 71-72, 1974.

[11] Y. H. Kiang, "Predicting Dew Points of Acid Gases," *Environment Energy Notes,* 2017.

[12] F. Habashi, Handbook of Extractive Metallurgy, Wiley-VCH,, 1997.

[13] S. B. V. Krishnan, Lurgi technical information C131 e, Lurgi, Frankfurt 1979.

[14] O. K. I. Barin, Thermodynamical properties of inorganic substances, Berlin: Springer Verlag, 1973.

[15] R. M. F. H. Kurushima, Min. Eng, Oct 1958.

[16] E. Wiklund, "Aufbereit. Tech. 18," 1977, pp. no. 6, 285-289.

[17] W. G. H. Wolf, "Chem. Ing. Tech. 40," 1968 nos.9/10, pp. 441-445.

[18] T. F. S. A. L. Renkey, "J. Met. 24," pp. no 6, 18-22, 1972.

[19] P. H. S. H. B. Andersson, "CIM Bull 75," vol. no. 845, pp. 172-177, 1982.

[20] E. M. H. W. G. Melcher, "Erzmetall 28," pp. nos. 7/8, 313-322, 1975.

[21] P. J. L. J. L. Leroy, Adv. Extr. Metall. Refin., London: Institution of mining and metallurgy, 1967.

[22] G. H. C. N. L. Mills, "Proc. Int. Symp. Extr. Metall. Copper I," 1976, pp. 458-487.

[23] G. L. Bassett, "Eng. Min. J 182," vol. no 9, pp. 102-103, 1982.

[24] S. B. S. Kellog, "Trans. Am. Inst. Min. Metall. Pet. Eng. 218," 1960, pp. no. 1, 70-81.

[25] H. W. A. Melin, "Erzmetall 20," 1967, pp. no. 12, 561-569.

[26] G. D. U. Sander, "Chem. Eng. Prog. 74," 1978, pp. no. 9, 57-67.

[27] H. v. P. R. S. K. Bodenbrenner, "Chem. Ing. Tech. 50," 1978, pp. no. 1, 30-36.

[28] N. Lowicki, "A new process for the recycling of waste sulphuric acids in Making the most of sulphuric acid," *Proc. Br. Sulphur Corp. 5th Int. Conf.,* pp. 401-409, 1981.

[29] W. J. Muller, "Angew. Chem. 38," 1925, pp. 794-795.

[30] P. R. A. Heitmann, "Chem. Ing. Tech. 46," 1974, pp. no. 14, 589-594.

[31] H. S. M. Beltran, "Use of two-stage Electrostatic precipitators in metallorgical roasting and sulphuric acid applications in Making the most of sulphuric acid," *Proc. Br. sulphur corp. 5th Conf.,* pp. 509-523, 1981.

[32] O. Sundstorm, "Sulfur 116," 1975, pp. 37-43.

[33] R. O. P. R. T. W. 7. P. Leckner, "Chem. Eng. Prog," 1982, pp. no 2, 65-70.

[34] J. B. P. J. M. Henderson, "Alche symp. ser. 72," 1977, pp. no 156, 69-73.

[35] G. R. A. C. D. S. J. 5. C. M. Yon, "Hydrocarbon Process," 1979, pp. no 7, 197-200.

[36] v. Chemieanlagen, Hoechst High Chem no.13, Dec. 1990.

[37] "Esseco Plants," A company of Esseco Industrial S.p.A., [Online]. Available: https://www.esseco.com/en/plants/.

[38] R. T. a. R. Sinnott, "Chemical Engineering Design, 2nd ed," Elsevier, 2013.

[39] R. E. AspenTech, Aspen Plus User Guide, Aspen Technology Inc..

[40] R. Smith, "Chemical Process Design and Integration," Wiley, 2005.

[41] R. W. R. a. L. G. B. R. M. Felder, Elementary Principles of Chemical Processes, 4th ed, Wiley, 2016.

[42] B. L. a. D. R. Vredeveld, " “Pinch Technology Has Come of Age,”," in *Chemical Engineering Progress*, 1984.

[43] Eastman, *Therminol 66 Heat Transfer Fluid Technical Data Sheet..*

[44] D. C. Company, *Dowtherm A Heat Transfer Fluid Technical Data Sheet.*

[45] D. C. Company, *Dowtherm T Heat Transfer Fluid Technical Data Sheet.*

[46] ExxonMobil, *Mobiltherm Heat Transfer Oils Product Data Sheet.*

[47] H. &. P. J. M. Renon, "Local compositions in thermodynamic excess functions for liquid mixtures," AIChE Journal, 14(1), , 1968, p. 135–144.

[48] R. &. K. R. Taylor, "Multicomponent Mass Transfer," Wiley, 1993.